GrundRisk - Coupling of vertical and horizontal transport models

Locatelli, Luca; Rosenberg, Louise; Bjerg, Poul Løgstrup; Binning, Philip John

Publication date:
2017

Document Version
Publisher's PDF, also known as Version of record

Ministry of Environment and Food of Denmark
Environmental Protection Agency

GrundRisk

Coupling of vertical and horizontal transport models

Environmental Project No. 1915

January 2017

Publisher: The Danish Environmental Protection Agency

Editors:
Luca Locatelli, DTU Miljø
Louise Rosenberg, DTU Miljø
Poul L. Bjerg, DTU Miljø
Philip J. Binning, DTU Miljø

ISBN: 978-87-93529-56-4

Content

Preface

This report presents the development of the GrundRisk model for contaminated site risk assessment. GrundRisk consists of 5 models, each simulating the contaminant transport from a contaminant source to an underlying aquifer. Each model consist of a vertical transport model (based on the models presented in Miljøstyrelsen (2016a)) coupled to a horizontal transport model (Miljøstyrelsen (2016b). This report focuses on the coupling between the vertical and horizontal models.

In order to achieve a more realistic risk assessment and prioritization of contaminated sites new methods need to be developed. This report is part of the project GrundRisk, where DTU Environment and Miljøstyrelsen (the Danish Environmental Protection Agency) have identified four research goals to be addressed in four sub-projects:

1. Development of an effective method for risk screening of identified contaminated sites (V1 and V2), so that contamination threatening groundwater resources is identified at an early stage.
2. Development of computational models for risk assessment of contaminated sites threatening groundwater resources. Based on an evaluation of the current risk assessment (standard no. 6 and 7, the Miljøstyrelsen, 1998), a new and more realistic model is developed for more detailed assessment following the initial risk screening.
3. Development of a methodology for prioritization of remediation measures in a groundwater catchment or a larger geographical area.
4. Development of a method to assess the groundwater management strategy.

This report is part of sub-project 2.

Konklusion og sammenfatning

I denne rapport præsenteres fem nye modeller (Model I, II, III, IV og V) til risikovurdering af forurenede grunde i Danmark. De nye modeller sammenkobler forskellige modeller for vertikal forureningstransport til en horisontal model for transport af forurening i grundvandet. Modellerne er baseret på stationære løsninger, og kan simulere forureningskoncentrationer under en forureningskilde og nedstrøms i et kontrolpunkt i det underliggende grundvandsmagasin. Modellerne er implementeret i MATLAB.

Denne rapport præsenterer de metoder, der er anvendt til at koble de vertikale og horisontale transportmodeller. Desuden beskrives det hvilke antagelser, der er gjort, og der gøres rede for baggrunden for de valgte metoder. Modellerne er desuden afprøvet på tre udvalgte testlokaliteter i Danmark for herigennem at demonstrere deres kunnen.

Ved anvendelse af de nye koblede modeller, der kobler den horisontale transportmodel GrundRisk (Miljøstyrelsen, 2016b) med vertikale transportmodeller, fås lavere forureningskoncentrationer i grundvandsmagasinet, end hvis den horisontale model anvendes alene. Dette skyldes, at modellerne indeholder flere transportprocesser for den vertikale transport (dispersion, nedbrydning mv.) under forureningens transport fra kilden til toppen af grundvandsmagasinet.

De nye modeller er en del af GrundRisk (Miljøstyrelsen, 2016b), som er et nyt risikovurderingsværktøj, der har til formål at give en mere realistisk risikovurdering, der inkluderer de mest relevante transportprocesser. Hermed bliver identifikationen af grundvandstruende forureninger mere præcis, og indsatsen i forhold til videre undersøgelser og afværge af forurenede lokaliteter bliver mere målrettet.

Anvendelsen af modellerne på de tre testlokaliteter viser, at vertikale transportprocesser kan have en betydelige indvirkning på de simulerede koncentrationer i det underliggende grundvandsmagasin, især når det gælder letnedbrydelige forureninger som eksempelvis benzen og toluen. Testlokaliteten Rugårdsvej, hvor grundvandsmagasinet er overlejret af homogent mættet sand, viste, at den 6 m lange vertikale transportvej fra forureningskilden til toppen af magasinet gav en koncentrationsreduktion for dichlorethylen (DCE), mens koncentrationer af nedbrydningsproduktet vinylklorid (VC) forøgedes. På testlokaliteten Vadsbyvej er grundvandsmagasinet overlejret af sprækket og mættet ler. Her viste resultaterne et lille fald i forureningskoncentrationerne under den 7 m lange vertikale transportvej fra forureningskilden til toppen af grundvandsmagasinet. Dette skyldes, at vandets hastighed i sprækkerne er høj, hvorfor transporttiden er lille og nedbrydningens omfang dermed også er lille. På lokaliteten MW Gjøes Vej overlejres et frit grundvandsmagasin af en 18 m dyb umættet zone af sand. Her viste resultaterne, at der under transporten til grundvandsmagasinet sker en lille reduktion i forureningskoncentrationer pga. gasdiffusion (der var ingen nedbrydning i den umættede zone). Denne testlokalitet blev også anvendt til at simulere en hypotetisk forurening med letnedbrydelige forureninger (benzen og toluen). Dette eksempel viste, at der skete en betydelig reduktion i forureningskoncentrationerne under transporten i den 18 m lange umættede zone især på grund af nedbrydning. Desuden blev der for MW Gjøes Vej simuleret en situation, hvor der antages ikke at ske infiltration til grundvandsmagasinet på grund af befæstningen af arealet. Dette eksempel illustrerede hvordan umættede og mættede transportprocesser påvirker forureningskoncentrationerne, når der ikke er nogen infiltration. Særligt viser eksemplet, hvorledes der sker diffusion af forureningen gennem kapillærzonen på grænsen mellem den umættede og den mættede zone.

Det er desuden undersøgt hvorledes modellernes følsomhed er overfor ændringer i infiltration, nedbrydningsrater og sprækkeafstande (som er blandt de mest betydende modelparametre). Beregningstiden for at simulere forureningskoncentrationer i et specifikt punkt i grundvandsmagasinet er få sekunder for Model I, II og V, hvorimod den kan vare op til 5 minutter for Model III og Model IV. Beregningstiden forøges næsten lineært med antallet af beregningspunkter i grundvandsmagasinet. At beregne et koncentrationsprofil i grundvandsmagasinet med 10 beregningspunkter vil tage ca. 50 minutter (10 gange 5 minutter) for hvert forureningsstof i Model III og Model IV (hvis der er en reaktionskæde med 4 stoffer vil det tage 4 gange 50 minutter).

De vertikale transportmodeller inkluderer de vigtigste processer, der påvirker transporten af forurening fra kildeområdet til et underliggende grundvandsmagasin. Der kan tages højde for forskellige typer af geologi. Resultaterne viser, at det er vigtigt at tage højde for den vertikale transport for at beskrive forureningsstoffernes skæbne fra forureningskilden til grundvandsmagasinet. Det er især vigtigt at give den vertikale transport opmærksomhed, hvis der er tale om forureningsstoffer, der nedbrydes forholdsvis let (f.eks. BTEX), mens det er mindre vigtigt for stoffer, der nedbrydes i mindre grad som f.eks. klorerede opløsningsmidler.

Summary and Conclusion

This report presents five new contaminant transport models (Model I, II, III, IV and V) for risk assessment of contaminated sites in Denmark. The new models couple different vertical contaminant transport models to a horizontal transport model. The models are based on steady-state solutions and can simulate the contaminant concentration below a contaminant source and downstream at control points in an underlying groundwater aquifer. The models are implemented in MATLAB.

This report presents the methods needed to couple the vertical and horizontal transport models, describing the assumptions made and the rationale for the chosen methods. The report demonstrates the capabilities of the new models by applying them to three selected case studies in Denmark.

The coupling between the horizontal transport model of GrundRisk (Miljøstyrelsen, 2016b) with vertical transport models produces a reduction in the modeled concentrations in the aquifer compared to the use of the horizontal transport alone. This is because of the added transport processes (dispersion, degradation, etc.) in the vertical direction from the contaminant source downward to the top of the aquifer.

The new models are part of GrundRisk (Miljøstyrelsen, 2016b) which is a new risk assessment tool that aims to achieve a more realistic risk assessment, including the most relevant transport processes so that identification of groundwater threatening contaminant sources becomes more precise and site remediation can be more targeted.

The model application to the Danish case studies shows that vertical transport processes can have a significant impact on the simulated concentration in underlying aquifers, particularly for highly degradable compounds such as benzene and toluene. The case study of Rugårdsvej where the aquifer is overlain by homogeneous saturated clay showed that the 6 m long vertical transport pathway from the source to the top of the aquifer reduced the initial concentrations of Dichlorethylen (DCE), however it increased those of Vinylchlorid (VC) (a degradation product formed from DCE). The case study of Vadsbyvej where the aquifer is overlain by fractured saturated clay showed that the 7 m long vertical transport pathway from the source to the top of the aquifer slightly reduces contaminant concentrations, because the water velocity in the fractures is high and the time it takes for the contaminant to reach the top of the aquifer from the source is short and thus the degradation is small. The case study of MW Gjøes Vej where the unconfined aquifer is overlain by unsaturated sand showed that the 18 m long vertical transport pathway from the source to the top of the aquifer slightly reduces contaminant concentrations due to gas diffusion (there was no degradation in the unsaturated zone). The case study of MW Gjøes Vej was also used to simulate a hypothetical scenario with highly degradable compounds (benzene and toluene) showing that the 18 m long vertical transport pathway from the source to the top of the aquifer significantly reduces contaminant concentrations mainly due to degradation. Furthermore, the case study of MW Gjøes Vej was simulated assuming no recharge in the area due to impervious surfaces covering the area. This scenario showed how unsaturated and saturated transport processes affect the contaminant concentrations when there is no recharge, particularly how the contaminant diffuses through the capillary fringe at the interface between the unsaturated and the saturated zone.

This report examined the model sensitivity to the model parameters: recharge rates, the first order degradation rates and fracture spacing (which are among the most influential model parameters).. The computational time to simulate the contaminant concentration at a single point in the aquifer is in the order of seconds for Model I, II and V, whereas it can be up to 5 minutes for Model III and Model IV. The computational time increases almost linearly with the number of simulated points in the aquifer, i.e. computing a concentration profile in the aquifer using 10 simulated points takes approximately 50 minutes (10 times 5 minutes) for each compound in Model III and Model IV (if there is a reaction chain of 4 compounds it will take 4 times 50 minutes).

The vertical transport model includes the main processes affecting contaminant transport from a source to an underlying groundwater aquifer. Various types of geology are considered. Consideration of vertical transport is shown to be important for determining the attenuation of contaminant transport between the source and the underlying aquifer. Attenuation during vertical transport is particularly important for more degradable compounds like BTEX, but has less effect for less degradable compounds like the chlorinated solvents.

1. Introduction

Risk assessments of contaminated sites are often conducted using simple models to determine contaminant concentrations in groundwater downstream of the contaminant source. In Denmark the JAGG model developed by Miljøstyrelsen (1998) and later updated (Miljøstyrelsen 2013) is widely used for risk assessments of contaminated sites. The JAGG model simulates the contaminant concentration at a point of compliance based on input source concentrations and geometry and other soil and groundwater parameters. JAGG is based on a simple 1-D model with many simplifying assumptions, and is usually employed assuming a worst case scenario. As a result of the conservative assumptions made, a large number of contaminant point sources have been identified as a potential problem for groundwater. Hence there is a need for improved models.

GrundRisk (Miljøstyrelsen, 2016b) is a new risk assessment tool that aims to achieve a more realistic risk assessment including the most relevant transport processes so that identification of groundwater threatening sources becomes more precise and site remediation can be more targeted.

This report presents the addition of a vertical transport model to the new GrundRisk contaminated site risk assessment model. Five models (I, II, III, IV and V) covering the most typical risk assessment situations are presented. Each of the five models couples a vertical transport model and a horizontal transport model (Figure 1). The vertical transport model simulates the contaminant concentration between the contaminant source and the top of the uppermost groundwater aquifer. The horizontal transport model simulates the subsequent transport and resulting concentrations in the aquifer. Each of the five models simulates the contaminant concentrations in the aquifer based on the input source concentration (Figure 1) and geometry and other unsaturated and saturated zone parameters.

The vertical transport models used in the five models are based on the work of Miljøstyrelsen (2016a), Chambon et al. (2011) and Troldborg et al. (2009), and the horizontal transport model was developed in Miljøstyrelsen (2016b). The vertical transport models include the processes of advection, hydrodynamic dispersion (mechanical dispersion + diffusion), sorption and degradation both for unsaturated and saturated conditions.

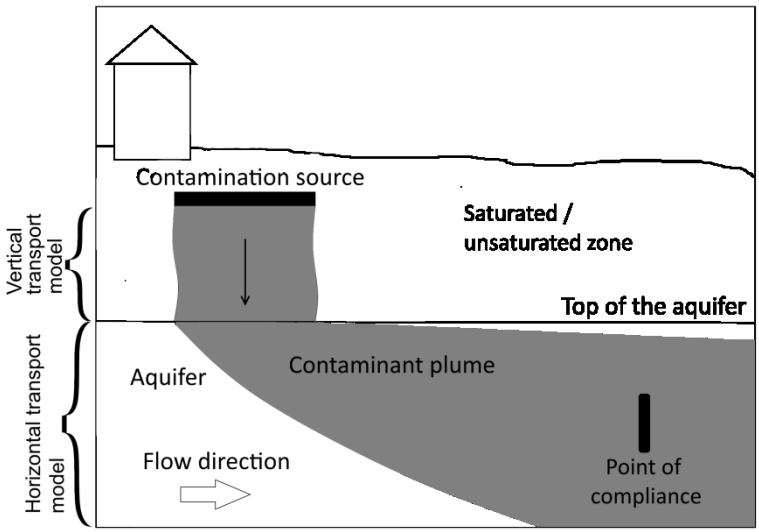

Figure 1. Conceptual figure showing the Grundrisk transport models. The models simulate the contaminant concentrations from the source downstream to a point of compliance in the aquifer. Each model couples a vertical and a horizontal transport model.

1.1 Aim of the project

This project aims to add a vertical transport model to GrundRisk (Miljøstyrelsen, 2016b), so that it can calculate both vertical transport from a source at a contaminated site down to the uppermost aquifer of significance, and then the horizontal transport downstream of the site in the uppermost aquifer. The vertical transport models should account for the changes in concentration occurring during vertical transport between the contaminant source and the top of the uppermost groundwater aquifer resulting from degradation and dispersive processes. A selection of vertical transport models is available in the Danish EPA reports of Miljøstyrelsen (2015) and Miljøstyrelsen (2016a), and the GrundRisk horizontal transport model is described in the Danish EPA report of Miljøstyrelsen (2016b).

In particular, this report aims to:

- Develop new and more realistic models for risk assessment of mapped V2 contaminated sites in Denmark.
- Select a set of vertical transport models from the Miljøstyrelsen reports (Miljøstyrelsen, 2015 and 2016a), to be used to describe the range of commonly encountered vertical transport scenarios.
- Develop the methods needed to couple the vertical and horizontal transport models, making clear the assumptions made and rationale for the methods chosen.
- Implement the coupled models in software Matlab.
- Demonstrate the new GrundRisk model capabilities by applying the models to contaminated sites in Denmark. In particular, the model applications should illustrate the main issues involved in the coupling of the vertical and horizontal transport models.

1.2 Model outputs

The new models simulate the contaminant water phase concentration from the source to the top of the aquifer and then horizontally downstream in the aquifer. Figure 2 shows examples of the output that can be obtained from the models simulating a contaminated site. Figure 2 (a) shows the simulated concentrations from the source to the top of the aquifer; Figure 2 (b) shows the simulated concentrations in the aquifer at a 0.01 m depth below the top of the aquifer (concentration along the centerline of the plume can also be plotted) and Figure 2 (c) shows the concentrations in the aquifer as a function of depth below the top of the aquifer, 100 m downstream the most downstream point of the source.

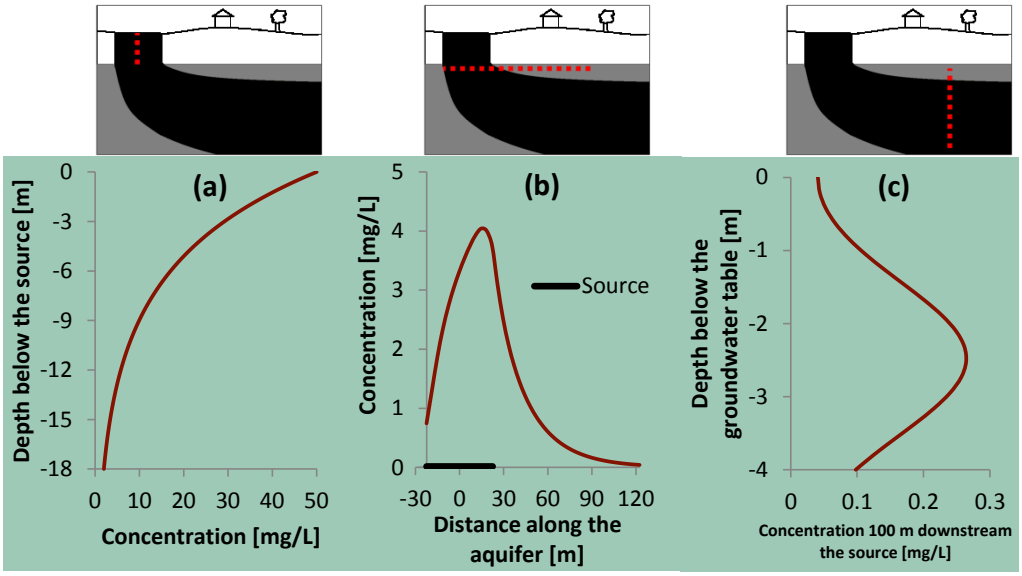

Figure 2. (a) Concentration as a function of the depth from the bottom of the source to the top of the aquifer. (b) Concentration in the aquifer as a function of the distance downstream of the source at a 0.01 m distance from the top of the aquifer. (c) Concentration in the aquifer at the centre of the plume 100 m downstream of the source.

1.3 Structure of the report

The report is organized as follows;

- Chapter 2 describes the details of the 5 different contaminant transport models. Conceptual model, mathematical description, coupling approach and an overview of the model parameters are given for each of the models.
- Chapter 3 presents the model applications to different case studies.

A first time reader of this report may wish to skip the mathematical details in chapter 2 and focus on the figures and conceptual descriptions of the models in chapter 2 and the model applications in chapter 3.

2. Description of the five contaminant transport models

This chapter describes the five different GrundRisk contaminant transport models (Model I, II, III, IV and V). Each model consists of a coupled vertical and a horizontal transport model simulating the transport from source to a point of compliance located in the aquifer downstream of the source zone. The vertical transport model equations and the coupling model between the vertical and horizontal transport components are described. A detailed description of the horizontal transport model can be found in Miljøstyrelsen (2016b). The five different models aim to include the most common contaminant transport mechanisms and processes of contaminated sites. Table 1 shows a summary of the five contaminant transport models.

Table 1. Summary of the 5 contaminant transport models included in this report.

	Model name	Model description
Model I	Homogeneous saturated clay overlying an aquifer	Contaminant transport from a source located in a homogeneous saturated clay, 1-D downward to the top of the aquifer and then 3-D horizontal transport in the aquifer.
Model II	Fractured saturated clay overlying an aquifer	Contaminant transport from a source located in a fractured saturated clay, 1-D downward to the top of the aquifer and then 3-D horizontal transport in the aquifer.
Model III	Unsaturated zone overlying an unconfined aquifer	Contaminant transport from a source located in the unsaturated zone, 3-D downward to the top of the aquifer and then 3-D horizontal transport in the aquifer.
Model IV	Unsaturated zone under an impervious area with zero infiltration	Contaminant transport from a source located in the unsaturated zone and below an impervious area, 3-D downward to the top of the aquifer and then 3-D horizontal transport in the aquifer.
Model V	Direct input from the source to the groundwater aquifer	3-D horizontal contaminant transport from a source, directly located at the top of the aquifer.

The choice of model is based on a conceptualization of the contaminant site which is outside the scope of this report. Each model is based on an analytical steady state solution of the 3-dimensional advection-dispersion equation and includes the most relevant transport processes for that specific case.

All the models are based on the following assumptions:

- Homogenous conditions. This means that the soil parameters (e.g. water content, porosity, bulk density, content of organic carbon and dispersivity) and contaminant parameters (e.g. diffusion coefficient, Henry's law constant and degradation rates) are constant in space and time.
- Linear, reversible, instantaneous equilibrium sorption processes between the water and solid phases
- Advection only occurs in the water phase and in one dimension (the vertical and/or horizontal flow direction) with a constant velocity.
- Degradation is described by 1st order kinetics and occurs in only the water phase.
- The concentration and the contaminant mass discharge in the contaminant source are constant over time.
- Transport of non-aqueous phase liquids is not included and the model only simulates dissolved compounds.

These assumptions/limitations are thought to be reasonable since the models are risk assessment tools and not advanced solute transport models. In order to ensure that the model can be used in risk assessments where little data is available, the conceptual models must be simple and the input parameters must be few and well-known.

Each model employs a different coordinate system in order to develop the needed analytical solution. Model I, II and V place the coordinate system origin on the upstream edge of the contaminant source, whereas Model III and IV place the origin at the center of the contaminant source.

2.1 Model I. Homogeneous saturated clay overlying an aquifer

The conceptual model for Model I is shown in Figure 3. Model I simulates the water phase concentrations in a saturated clay between the contaminant source and an underlying aquifer using a vertical transport model, and then the concentrations in the underlying aquifer using a horizontal transport model. The contaminant source is considered to have length L_x, width L_y, and a source concentration of C_0. The source can be located below land surface and has a user specified distance to the top of the aquifer. The vertical transport model of Model I simulates the concentrations between the contaminant source and the top of the aquifer using a 1D steady-state analytical solution that assumes that the horizontal mixing (dispersion) is negligible (i.e. there is no variation in concentrations in the *y* and *x* directions of the vertical transport).

The output of the vertical transport model is the concentration C_1 at the top of the aquifer. The concentration C_1 is used as input to the horizontal model computing downstream concentrations in the aquifer. In the horizontal transport model, the concentration C_1 is applied over the same area (L_xL_y) as used in the source area. The horizontal model simulates the concentrations in the aquifer based on a 3D steady-state analytical solution that includes advection and dispersion in the aquifer. A complete description of the horizontal transport model is found in Miljøstyrelsen (2016b). The following 3 sections describe the vertical transport component of Model I, the coupling between the vertical and the horizontal transport models, and the model parameters.

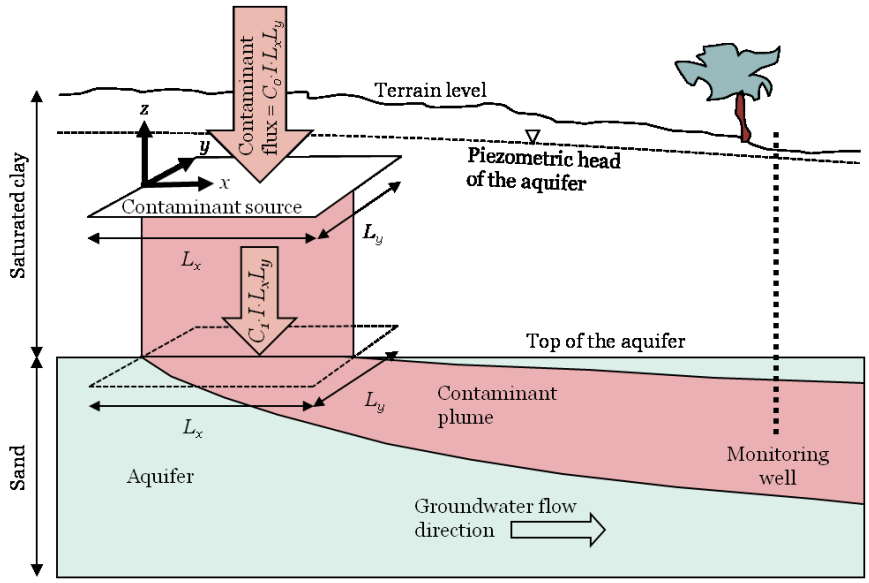

Figure 3. Conceptual Model I. Vertical contaminant transport from a source located in a HOMOGENEOUS saturated clay, downward to the top of the aquifer and then horizontal transport in the aquifer.

2.1.1 Model I. Homogeneous saturated clay vertical contaminant transport model

This section presents the steady-state analytical solution that is used for computing the vertical transport in Model I. The clay layer in this case is saturated (Figure 3) and so there is no gas transport. The most significant transport processes within a homogeneous saturated layer are percolation (advection) of the contaminant with groundwater recharge; diffusion and mechanical dispersion in the water phase; sorption; and degradation. Note that Figure 3 shows that the water table is above the contaminant source. The model can also be used when the water table is below the source because the porous media will still be saturated above the aquifer due to capillary rise in the low permeability material.

The transport equation for Model I is (Miljøstyrelsen, 2016a):

$$R\frac{\partial C_w}{\partial t} = D_w \nabla^2 C_w - v\frac{\partial C_w}{\partial z} - \lambda C_w$$

t	TIME
λ	FIRST ORDER DEGRADATION RATE
C_W	CONCENTRATION IN THE WATER PHASE
Z	VERTICAL DISTANCE FROM THE SOURCE
v	PORE WATER VELOCITY IN THE Z DIRECTION
R	RETARDATION FACTOR
D_W	HYDRODYNAMIC DISPERSION COEFFICIENT IN WATER

Equation 1

The one-dimensional steady-state solution is shown in Equation 1 (van Genuchten et al., 1982). It is noted that the retardation factor *R* does not affect the steady-state vertical transport. However, it can affect contaminant concentration at the top of the aquifer where the output of the vertical transport model is input into the horizontal transport model (see Appendix I). This solution was found by applying the boundary conditions of fixed concentration at the source $c(0)=C_o$ and zero gradient at infinite distance from the source $dc/dz(\infty)=0$. The 1D solution has been shown to be a good approximation of the 3D solution (Miljøstyrelsen, 2016a) because transverse dispersion is negligible in saturated clay. Equation 2 is used to calculate the water phase concentration at the top of the uppermost aquifer underlying the source. This concentration is then used as input to the horizontal transport model.

$$c(z) = C_0 \exp\left(\frac{(v-u_u)z}{2D_z}\right)$$

$$u_u = v\left(1+\frac{4\lambda D_z}{v^2}\right)^{1/2}$$

$$D_z = v\alpha_L + D_w^*$$

C0	INITIAL WATER CONCENTRATION
z	VERTICAL DISTANCE FROM THE SOURCE
v	PORE WATER VELOCITY IN THE Z DIRECTION
λ	FIRST ORDER DEGRADATION RATE
D_Z	HYDRODYNAMIC DISPERSION COEFFICIENT IN WATER
D_W	EFFECTIVE DIFFUSION COEFFICIENT IN WATER
α_L	LONGITUDINAL DISPERSIVITY

Equation 2

2.1.2 Model I. Coupling between the horizontal and vertical model

The conceptual model used for coupling the vertical and the horizontal transport model is shown in Figure 3. The horizontal transport model (Miljøstyrelsen, 2016b) requires the input area parameters L_x *and* L_y, the concentration C_1 and the infiltration flux *I*. The source area for the horizontal model is assumed to be the same as the source area of the vertical model (L_x *and* L_y do not change); the concentration C_1 is found by Equation 2 at the user specified distance between the contaminant source and the top of the aquifer; and the water infiltration flux is assumed to be constant. The area at the top of the aquifer is assumed to be the same as that of the source because transverse mixing processes are small in a clay aquitard.

When coupling the vertical and horizontal transport models, it is important to consider how concentrations change as the contaminant crosses between the aquitard (vertical transport) and aquifer (horizontal transport). At the point between the two materials, there might be a jump in total concentrations (total contaminant mass/volume) at steady-state because of the change in sorption characteristics between materials (see Appendix I). However, there is no jump in water phase concentrations. Details about the effect of contaminant transport simulations across different soil layers (with different sorption characteristics) are provided in Appendix I.

2.1.3 Model I. Model parameters, variables and output

Table 2 shows the user input model parameters and Table 3 the derived variables for Model I. The input parameters and variables in the tables are divided into three categories: Global parameters applicable to both the vertical and the horizontal transport model, Vertical model parameters, and Horizontal Model parameters. The model output is the contaminant concentration at a single or multiple user specified points in the underlying aquifer.

Table 2. User input parameters of Model I

	Input parameter	Description
Global parameters	Y_i [-]*	Stoichiometric ratio of each compound i of the degradation chain
	I [L/T]	Recharge
	Lx [L]	Source length
	Ly [L]	Source width
Vertical model	C_0_v [M/L^3]	Concentration in the water phase at the source
	k_v [T-1]	First order degradation rate
	n_v [-]	Porosity = water content (assuming full water saturation)
	α_L_v [L]	Longitudinal dispersivity (z direction)
	Z_v [L]	Distance between the source and the top of the aquifer
	Dw_v [L^2/T]	Free diffusion coefficient in water
Horizontal model	H [L]	Thickness of the aquifer
	u [L/T]	Groundwater velocity
	k [T^{-1}]	First order degradation rate
	n [-]	Porosity
	α_L [L]	Longitudinal dispersivity (x direction)
	α_T [L]	Transversal dispersivity (y direction)
	α_V [L]	Vertical dispersivity (z direction)

*** Y_{i+1}=molar mass^{i}/molar mass^{i+1}. It is the ratio of the molar masses of the compounds in a degradation chain.**

Table 3. Derived variables for Model I.

	Derived variables	Description
Vertical model	$v_{\_v} = \frac{I}{n}$	Pore water velocity
	$D^*_{w\_v} = \tau D_{w\_v}$	Effective diffusion coefficient in water (Bear, 1972)
	τ	Tortuosity of the soil matrix. Assumed to equal to the soil porosity as a first approximation (Parker et al., 1994)
Horizontal model	$D_L = \alpha_L u$	Longitudinal dispersion coefficient
	$D_T = \alpha_T u$	Transversal dispersion coefficient
	$D_V = \alpha_V u$	Vertical dispersion coefficient

2.2 Model II. Fractured saturated clay overlying an aquifer

Figure 4 shows the conceptual model for Model II. Model II simulates the water phase concentration in saturated fractured clay layer using the vertical transport model of Chambon et al. (2011) and Miljøstyrelsen (2009a), and then the concentrations into the aquifer using the horizontal model of Miljøstyrelsen (2016b). The contaminant source is represented by the user specified length L_x, the width L_y, and the source concentrations C_0. The source can be located below terrain and is located at a user specified distance from the top of the aquifer. The vertical transport Model II simulates the concentrations from the contaminant source to the top of the aquifer assuming that the advective contaminant flux from the source ($C_0 \cdot I \cdot Lx \cdot Ly$) is entirely conveyed through vertical parallel (equally distanced) fractures separated by a distance *2B* and with fracture thickness (aperture) of *2b (*see Figure 4). The vertical model is based on a 1D steady-state analytical solution of the transport equation assuming advective transport in the fractures and diffusive transport in the matrix. At the bottom of the fractures (the top of the aquifer), fully mixed conditions (a homogeneous distribution) over the area L_xL_y are assumed. The validity of this assumption, together with different possible fracture orientations are discussed in the example shown in Section 3.2.6.

The vertical transport model simulates the concentration C_1 at the top of the aquifer. This concentration is then used as input to the horizontal model to simulate the concentrations in the aquifer. The concentration C_1 is applied (similarly to Model I) to the horizontal model assuming that the source area (L_xL_y) is the same as the input source area of the vertical model at the contaminant source. The horizontal model simulates the concentrations in the aquifer with a 3D steady-state analytical solution that includes advection and dispersion in the aquifer. A 2D steady-state analytical solution is used when the aquifer has a small thickness. A complete description of the horizontal transport model is found in Miljøstyrelsen, 2016b. The following 3 sections describe the vertical transport model of Model II, the coupling between the vertical and the horizontal transport models, and the model parameters.

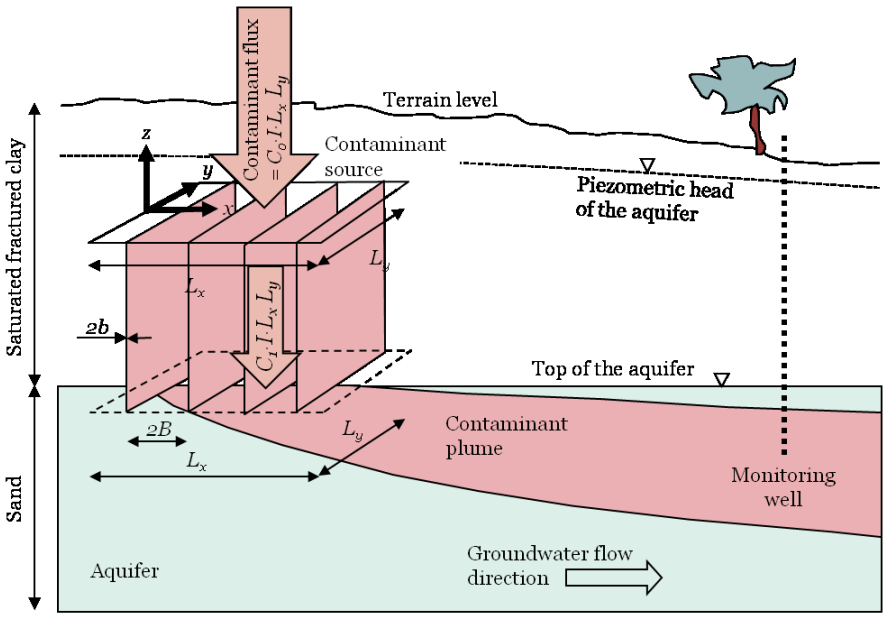

Figure 4. Conceptual model II. Contaminant transport from a source located in a fractured saturated clay, downward to the top of the aquifer and then horizontal transport in the aquifer.

2.2.1 Model II. Vertical transport model within a saturated fracture clay.

The vertical transport model of Model II calculates the downward vertical contaminant transport in a saturated fractured clay from the source to the top of the underlying aquifer in a saturated fractured clay. The model was presented by Chambon et al. (2011). The contaminant transport in fractured clays is controlled by advection in the fractures and diffusion in the matrix (Chambon et al., 2011). Contamination in both the fractures and the matrix is affected by both sorption and degradation (Jørgensen et al., 2004; McKay et al., 1993; Broholm et al., 2000).

Several different mathematical models describing the contaminant transport in fractured media are described by Chambon et al. (2011). Model II employs the model with a constant source concentration above the fractured soil (Chambon et al. 2011). The vertical transport model used in Model II is illustrated in Figure 5; this model simulates the steady-state concentration in the fractured clay from a source with constant concentration C_0. The mathematical model is based on the following assumptions (in addition to those already mentioned in the introduction to Chapter 2): mass transport along the fracture is one-dimensional; dispersion along the fracture is neglected; advection in the porous matrix is neglected; transport in the matrix is perpendicular to the fracture. The mathematical solution was developed for an infinitly long single fracture conveying the water flux over on infinitely long strip of width *2B*.

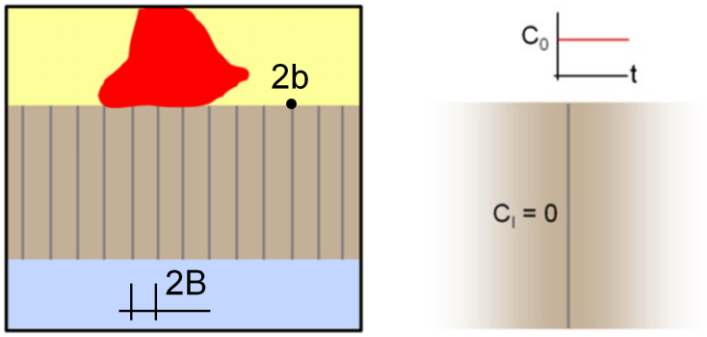

Figure 5. Conceptual sketch of the vertical model of model II. source overlying the fractured media for an infinite time (Chambon et al., 2011). C_0 is the input concentration, c_I is the initial concentration in the matrix, 2b is the fracture spacing and 2b is the fracture aperture. the red area represents the source above the fractured clay (modified from Chambon et al., 2011).

The one-dimensional transport equation in a vertical fracture is shown in Equation 3 (Tang et al., 1981). Advective transport is only considered in the fractures since there is little advection in the matrix. This approximation is reasonable if the hydraulic conductivity of the matrix is low compared to the hydraulic conductivity of the fracture.

$$R_f \frac{\partial C_f}{\partial t} + v_f \frac{\partial C_f}{\partial z} + \frac{Q_m}{b} + \lambda C_f = 0$$

t	TIME
λ	FIRST ORDER DEGRADATION RATE
C_f	CONCENTRATION IN THE WATER PHASE IN A FRACTURE
z	VERTICAL DISTANCE FROM THE SOURCE
v_f	WATER VELOCITY IN THE FRACTURE
R_f	RETARDATION FACTOR ON THE FRACTURE SURFACE
Q_m	MASS TRANSFER FLUX AT THE FRACTURE-MATRIX INTERFACE [M/T/L2]
b	HALF APERTURE OF THE FRACTURE

Equation 3

The steady-state solution is given in Equation 4
(Chambon et al., 2011). This equation was obtained by applying the initial conditions of zero initial concentration $C_f(z,o)=0$ and the boundary condition of zero concentration at infinite distance from the source $C_f(\infty,t)=0$.

$$C_f(z) = C_0 \exp\left(-\frac{\lambda z}{v_f}\right)\exp\left(-\frac{H\sqrt{\frac{\lambda}{R_m}}}{A}\right)$$

$$H = \frac{R_f z}{v_f}$$

$$A = \frac{bR_f}{n\sqrt{R_m D_m}}$$

$$D_m = \tau D_d$$

$$R_m = 1 + \frac{\rho_b}{n} K_d$$

$$\rho_b = \rho_s (1-n)$$

t	TIME
λ	FIRST ORDER DEGRADATION RATE
C_f	CONCENTRATION IN THE FRACTURE
C_0	INITIAL CONCENTRATION
z	VERTICAL DISTANCE FROM THE SOURCE
v_f	WATER VELOCITY IN THE FRACTURE
ρ_b	BULK DENSITY
ρs	DENSITY OF MINERAL PARTICLES (2650 kg/m^3)
R_f	RETARDATION FACTOR ON THE FRACTURE SURFACE. ASSUMED TO EQUAL RM (JØRGENSEN ET AL., 1998, 2002)
R_m	RETARDATION FACTOR ON THE MATRIX
D_m	EFFECTIVE DIFFUSION COEFFICIENT IN WATER IN THE MATRIX
Dd	FREE DIFFUSION COEFFICIENT IN WATER
τ	MATRIX TORTUOSITY (ASSUMED TO EQUAL THE POROSITY AS A FIRST APPROXI MATION (PARKER ET AL., 1994))
B	HALF APERTURE OF THE FRACTURES
n	POROSITY
θw	WATER CONTENT ASSUMED TO EQUAL POROSITY
K_d	SORPTION COEFFICIENT

Equation 4

The water velocity in the fractures v_f is calculated using Equation 5. Assuming that the hydraulic conductivity for the clay matrix is very low (generally in the order of 10^{-10} m/s (Jørgensen et al., 2002)), the average fracture aperture *2b* (see Figure 4) is calculated from the bulk hydraulic conductivity K_b and the spacing between two vertical fractures *2B* (Mckay et al. 1993). Equation 5 contains 5 parameters (K_b, *2b*, *2B*, *I* and *i*), but only 3 must be defined in order to ensure physical consistency between the 5 parameters. The user should specify the recharge *I*; the spacing between the fractures *2B;* and either the bulk hydraulic conductivity K_b or the fracture aperture *2b*. The model then calculates the remaining parameters (see Chambon et al. (2011) for details).

$$v_f = (2b)^2 \frac{\rho g}{12\mu} i$$

$$2b = \left(K_b 2B \frac{12\mu}{\rho g} \right)^{1/3}$$

$$K_b = \frac{I}{i}$$

K_b	BULK HYDRAULIC CONDUCTIVITY [m/s]
μ	VISCOSITY [Pa·s]
2B	SPACING BETWEEN FRACTURES [m]
2B	FRACTURE APERTURE [m]
ρ	DENSITY OF THE WATER [kg/m^3]
g	GRAVITATIONAL ACCELERATION [m/s^2]
I	RECHARGE [m/s]
i	HYDRAULIC GRADIENT GRADIENT [-]

Equation 5

Model II limitations

There are some limitations to Model II (Chambon et al. 2011): (1) the tool is not suitable for highly fractured media, with small average fracture spacing (*2B < 1-1.5 m*) (an equivalent porous media model such as Model I can be used for fracture spacing of less than 40 cm); (2) the validity of the single fracture assumption is controlled by the diffusion time from the fracture to the middle of the porous matrix, which can be characterized by $R_m B^2/D_m$ (*Rm*= retardation factor on the matrix; *B*= half spacing between fractures; *Dm*= effective diffusion coefficient in water in the matrix). If this diffusion time is high compared to the leaching time considered (the leaching time is the ratio between the vertical transport distance and the velocity in the fracture), the assumption of single fracture is reasonable (an equivalent porous media model such as Model I can be used if the assumption is not reasonable); (3) diffusion is assumed to be the dominant process in the porous matrix, so the model is applicable to low-permeability deposits only (such as clayey tills); (4) some studies showed that degradation occurs preferentially in and around high permeability zones especially when the transport of bacteria, reactants or nutrient is limited by diffusion (Hønning et al., 2007; Scheutz et al., 2010) and/or by pore size exclusion (Lima et al., 2007). In such cases the attenuation due to degradation will be largely overestimated by Model II since it assumes degradation both in the fractures and in the matrix (Chambon et al., 2011).

2.2.2 Model II. Coupling between the horizontal and vertical model

The conceptual model for Model II is shown in Figure 4. The horizontal transport model requires the input area parameters L_x *and* L_y, the concentration C_1 and the infiltration flux *I*. It is assumed that there is complete mixing of the contaminant mass over the area $L_x L_y$ at the bottom of the fractured medium; the concentration C_1 at the top of the aquifer is found by the vertical model Equation 4. The contaminant flux area at the top of the aquifer (input to the horizontal model) is assumed to be the same as the source area of the vertical model ($L_x L_y$) and the recharge flux *I* is also assumed to be the same. The area does not change between the source and the bottom of the clay layer because horizontal spreading (lateral dispersion) in the clay is small. The diffusive flux from the clay interface at the bottom of the aquitard into the aquifer is assumed to be small and so it is not considered.

Section 3.2.6 further discusses the assumption of fully mixed conditions at the top of the aquifer. A COMSOL Multiphysics model was setup to check this assumption. The assumption of fully mixed conditions at the bottom of the fractures slightly underestimates the simulated contaminant concentration at the point of compliance 100m downstream of the source. The assumption is therefore considered to be reasonable.

When coupling the vertical and horizontal transport models, it is important to consider how concentrations change as the contaminant crosses between the aquitard (vertical transport) and aquifer (horizontal transport). This issue is handled in the same way as for Model I.

2.2.3 Model II. Model parameters and output

Table 4 shows the user input model parameters for Model II. The input parameters and variables in the tables are divided into three categories: Global parameters, Vertical model and Horizontal Model. The Model II output is the contaminant concentration at a single or multiple user specified points in the underlying aquifer.

Table 4. User input parameters of Model II

	Input parameter	Description
Global parameters	Y_i [-]*	Stoichiometric ratio of each compound i of the degradation chain
	I [L/T]	Recharge
	L_x [L]	Source length
	L_y [L]	Source width
Vertical model	$C_{0\ v}$ [M/L^3]	Concentration
	$K_{\_v}$ [T^{-1}]	First order degradation rate
	$n_{\_v}$ [-]	Porosity = water content
	α_{L_v} [L]	Longitudinal dispersivity (z direction)
	$Z_{\ v}$ [L]	Distance between the source and the top of the aquifer
	$D_{w\ v}$ [L^2/T]	Free diffusion coefficient in water
	$2B_{\ v}$ [L]	Fracture spacing
	b [L]	Fracture aperture
	$K_{b\ v}$ [M/L]	Bulk hydraulic conductivity
	K_{d_v} [L^3/M]	Sorption coefficient
Horizontal model	H [L]	Thickness of the aquifer
	u [L/T]	Groundwater velocity
	k [T^{-1}]	First order degradation rate
	n [-]	Porosity
	α_L [L]	Longitudinal dispersivity (x direction)
	α_T [L]	Transversal dispersivity (y direction)
	α_V [L]	Vertical dispersivity (z direction)

**** Y_{i+1}=molar mass^i/molar mass^{i+1}. It is the ratio of the molar masses of the compounds in a degradation chain.***

2.3 Model III. Unsaturated zone overlying an unconfined aquifer

The conceptual model of Model III is shown in Figure 6. Model III simulates the water phase concentrations in the unsaturated zone overlying an unconfined aquifer using a downward vertical transport model and then the concentrations in the aquifer using a horizontal transport model. The contaminant source is represented by the length L_x, the width L_y and the source concentration C_0. The source can be located below terrain and is located at a user specified distance from the top of the aquifer. The vertical transport model of Model III simulates the water phase concentrations from the contaminant source to the top of the aquifer using a 3D steady-state analytical solution.

The vertical transport model simulates the concentration $C_1(x,y,Zv)$ at the top of the aquifer which is then used as input to the horizontal model to simulate the concentrations in the aquifer. The concentration $C_1(x,y,Zv)$ is integrated over the x and y area at the groundwater table level (Zv) and multiplied by the recharge rate I to obtain the contaminant mass input for the horizontal model. The horizontal model simulates the concentrations in the aquifer using a 3D steady-state analytical solution including advection and dispersion in the aquifer. The horizontal model is a modified version of the horizontal model shown in Miljøstyrelsen (2016b) to account for a larger contaminant discharge area at the groundwater table. The following sections describe the vertical component of Model III, the coupling between the vertical and the horizontal transport models, the horizontal model and the model parameters.

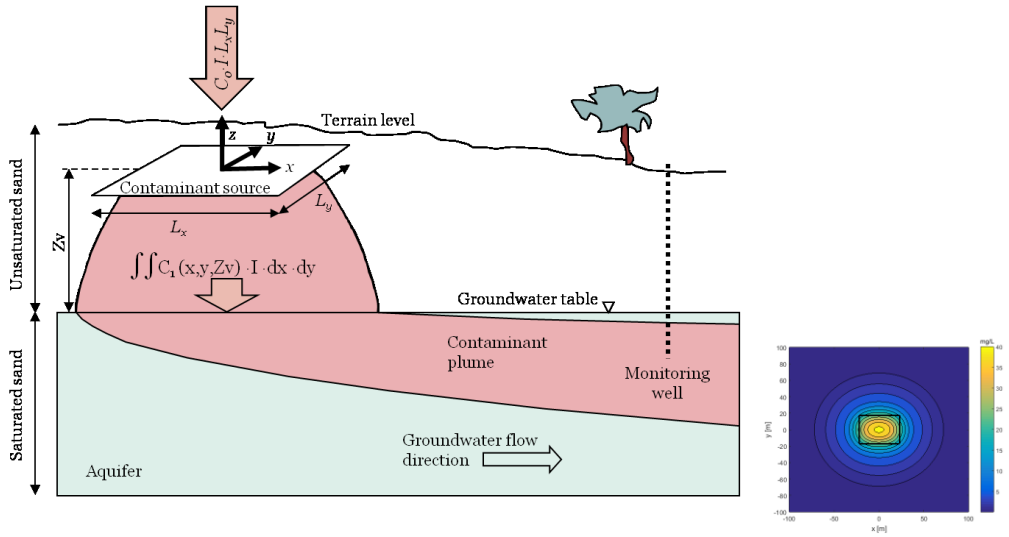

Figure 6. (Left) Conceptual model III. Contaminant transport from a source located in the unsaturated zone, downward to the top of the aquifer and then horizontal transport in the aquifer. (Right) Concentration at the top of the aquifer in plan view as a function of x and y (z_v=18 m); the black line shows the location of the contaminant source (from the Mw Gjøes Vej model application).

2.3.1 Model III. Unsaturated zone vertical transport model with infiltration

The vertical model of Model III simulates the downward vertical contaminant transport in the water phase in the unsaturated zone when the recharge is greater than zero. Contaminants are transported in both the air and water phases. Diffusion is considered in the air phase, but not in the water phase because vapour phase diffusion is several orders of magnitude larger than that occurring in the aqueous phase (approximately 10^4 times larger. See Schwarzenbach et al., 1993). Advection is considered in the water phase due to water infiltration, but air phase advection is typically small and so is neglected.

Gas transport is a significant process in the unsaturated zone. Many studies have shown that diffusion in the gas phase is a dominant transport process in the unsaturated zone, particularly for volatile compounds (Christophersen et al., 2005). Both field data and model results show that the risk of contamination of groundwater consisting of volatile compounds is limited in areas in contact with the atmosphere due to diffusive transport and loss to the atmosphere (Christophersen et al., 2005; Lahvis et al., 2004; Grathwohl et al., 2002; Lahvis et al., 2000).

By summing the transport equations for water and air and employing the phase partitioning expression $C_a=K_H \cdot C_w$, Equation 6 is obtained.

$$\frac{\partial(R\theta_w + K_H\theta_a)C_w}{\partial t} = \nabla(\theta_w \mathsf{D}_w + \theta_a K_H \mathsf{D}_a)\nabla C_w - q_w \frac{\partial C_w}{\partial z} - \theta_w \lambda C_w$$

Cw	CONCENTRATION IN THE WATER
R	RETARDATION FACTOR
K_H	DIMENSIONLESS HENRY'S LAW CONSTANT
θw	WATER CONTENT
θa	AIR CONTENT
t	TIME
q_w	DARCY'S FLUX
D_w	HYDRODYNAMIC DISPERSION IN WATER
D_a	HYDRODYNAMIC DISPERSION IN AIR
λ	FIRST ORDER DEGRADATION RATE IN THE WATER PHASE

Equation 6

The 3D steady-state solution of Model III is given by Equation 7 (Miljøstyrelsen, 2016a; Troldborg, 2009). This equation was obtained with boundary and initial conditions describing a source of concentration perpendicular to the flow direction ($C_w(x,y,0,t)=C_0$ for $-L_x/2<x<L_x/2$ and $-L_x/2<x<L_x/2$; $C_w(x,y,0,t)=C_0$ otherwise) and a zero concentration initial condition $C_w(z,y,z,0)=0$.

$$C_w(z,x,y,t) = \frac{C_0}{8} \int_{\tau=0}^{\infty} f_z'(z,\tau) f_x'(x,\tau) f_y'(y,\tau) d\tau$$

where:

$$f_z'(z,\tau) = \frac{z}{\sqrt{\pi D_z}} \exp\left(\frac{vz}{2D_z}\right) \cdot \exp\left[-\tau\left(\frac{v^2}{4D_z} + \lambda'\right) - \frac{z^2}{4D_z\tau}\right] \cdot \tau^{-3/2}$$

$$f_x'(x,\tau) = \left\{ erf\left[\frac{x + \frac{L_x}{2}}{2\sqrt{D_x\tau}}\right] - erf\left[\frac{x - \frac{L_x}{2}}{2\sqrt{D_x\tau}}\right] \right\}$$

$$f_y'(y,\tau) = \left\{ erf\left[\frac{y + \frac{L_y}{2}}{2\sqrt{D_y\tau}}\right] - erf\left[\frac{y - \frac{L_y}{2}}{2\sqrt{D_y\tau}}\right] \right\}$$

$$v = \frac{I}{\theta_w}$$

$$R' = R\theta_w + \theta_a K_H$$

$$\lambda' = \frac{\theta_w \lambda}{R'}$$

$$R = 1 + \frac{\rho_b}{\theta_w} K_d$$

$$\rho_b = \rho_s (1 - n)$$

$$K_d = f_{oc} K_{oc}$$

$$D_x = D_y = \frac{\theta_w \alpha_T v + \theta_w D_w^* + \theta_a D_a^* K_H}{R'}$$

$$D_z = \frac{\theta_w \alpha_L v + \theta_w D_w^* + \theta_a D_a^* K_H}{R'}$$

$$D_a^* = D_{d,a} \frac{\theta_a^{2,5}}{n}$$

$$D_w^* = D_a^* \cdot 10^{-4}$$

Cw	CONCENTRATION IN THE WATER PHASE
t	TIME
C0	CONCENTRATION IN THE SOURCE
I	RECHARGE
erf	ERROR FUNCTION
L_X	LENGTH OF THE SOURCE
L_Y	WIDTH OF THE SOURCE
n	POROSITY
ρ_b	BULK DENSITY
ρs	DENSITY OF MINERAL PARTICLES (2650 kg/m^3)
Z	VERTICAL DISTANCE FROM THE SOURCE
K_H	DIMENSIONLESS HENRY'S LAW CONSTANT
θw	WATER CONTENT
θa	AIR CONTENT
v	PORE WATER VELOCITY
$D_{d,a}$	FREE DIFFUSION COEFFICIENT IN AIR
Da*	EFFECTIVE DIFFUSION COEFFICIENT IN AIR
Dw*	EFFECTIVE DIFFUSION COEFFICIENT IN WATER
α_L	LONGITUDINAL DISPERSIVITY IN THE WATER PHASE
α_T	TRANSVERSAL DISPERSIVITY IN THE WATER PHASE
f_{oc}	FRACTION OF ORGANIC CARBON
K_{oc}	PARTITION COEFFICIENT WITH RESPECT TO ORGANIC MATTER
λ	FIRST ORDER DEGRADATION RATE

Equation 7

2.3.2 Model III. Coupling between the horizontal and vertical model

The conceptual model describing the coupling between the vertical and the horizontal transport models is shown in Figure 6.

The vertical transport model simulates steady-state spatially distributed concentration $C_1(x,y,Zv)$ (Equation 7) at the top of the aquifer. The spatially distributed concentration at the top of the aquifer $C_1(x,y,Zv)$ is integrated over x and y and multiplied by the recharge rate in order to obtain the contaminant mass discharge input to the horizontal model.

The steady-state solution (Equation 8) for the horizontal transport model is that of Miljøstyrelsen (2016b). Equation 8 is similar to the solution of Miljøstyrelsen (2016b) (that is used on Model I, II and V) but with 2 changes: (1) the mass flux [M/L^2/T] from a point source at the top of the aquifer is now described by the function $J(x',y')$; (2) the integrals are calculated from -∞ to +∞, because the contaminated area above the top of the aquifer is now larger than the original source area.

The integrals are solved numerically over a finite integration interval. The integration interval was set from $-10max(L_x,L_y)$ to $10max(L_x,L_y)$. The integration interval selected based on a different scenarios applied to the case study of MW Gjøes Vej (see Section 3.3.6). This selected integration interval is assumed to be ok for other cases. The integration interval was selected large enough so that almost 100% of the contaminant flux to the aquifer was captured. The selection was made after testing several integration intervals in different scenarios that included also very diffusive compounds.

$$c(x,y,z) = \int_{-\infty}^{\infty}\int_{-\infty}^{\infty} \frac{2J(x',y')}{4\pi n\gamma\sqrt{D_y D_z}} \exp\left(\frac{u(x-x')}{2D_x} - \frac{\beta\gamma}{2D_x}\right) dx'\,dy'$$

$$J(x',y') = C_1(x',y',Z_v)I$$

$$\beta = \left(u^2 + 4D_x\lambda\right)^{1/2}$$

$$\gamma^2 = (x-x')^2 + \frac{D_x}{D_y}(y-y')^2 + \frac{D_x}{D_z}z^2$$

$$D_x = \alpha_L u$$

$$D_y = \alpha_T u$$

$$D_z = \alpha_V u$$

C1	WATER PHASE CONCENTRATION AT THE TOP OF THE AQUIFER (OUTPUT OF THE VERTICAL TRANSPORT MODEL)
z	DEPTH BELOW THE TOP OF THE AQUIFER
Z_V	DISTANCE BETWEEN THE CONTAMINANT SOURCE AND THE TOP OF THE AQUIFER
I	RECHARGE
n	POROSITY
α_T	TRANSVERSAL DISPERSIVITY IN THE WATER PHASE
α_L	LONGITUDINAL DISPERSIVITY IN THE WATER PHASE
α_V	VERTICAL DISPERSIVITY IN THE WATER PHASE
D_X	DISPERSION COEFFICIENT IN THE X DIRECTION (LONGITUDINAL)
D_Y	DISPERSION COEFFICIENT IN THE Y DIRECTION (TRANSVERSAL)
D_Z	DISPERSION COEFFICIENT IN THE Z DIRECTION (TRANSVERSAL)
λ	FIRST ORDER DEGRADATION RATE
u	GROUNDWATER VELOCITY IN THE X DIRECTION

Equation 8

2.3.3 Model III. Model parameters and output

Table 5 shows the user input model parameters for Model III. The input parameters and variables in the tables are divided into three groups: Global parameters, Vertical model and Horizontal Model. The Model III output is the contaminant concentration at a single or multiple user specified points x, y, z.

Table 5. User input parameters of Model III

	Input parameter	Description
Global parameters	Y_i [-]*	Stoichiometric ratio of each compound i of the degradation chain
	I [L/T]	Recharge
	L_x [L]	Source length
	L_y [L]	Source width
Vertical model	$C_{0\ v}$ [M/L^3]	Concentration
	$k_{\ v}$ [T^{-1}]	First order degradation rate
	$n_{\ v}$ [-]	Porosity = water content
	$\theta_{w\ v}$ [-]	Water content
	α_{L_v} [L]	Longitudinal dispersivity (z direction)
	α_{T_v} [L]	Transversal dispersivity (z direction)
	$Z_{\ v}$ [L]	Distance between the source and the top of the aquifer
	$D_{a\ v}$ [L^2/T]	Free diffusion coefficient of air
	K_H [-]	Dimensionless Henry's law constant
	$foc_{\ v}$ [-]	Fraction of organic carbon
	K_{oc_v} [-]	Partition coefficient with respect to organic matter
Horizontal model	H [L]	Thickness of the aquifer
	u [L/T]	Groundwater velocity
	k [T^{-1}]	First order degradation rate
	n [-]	Porosity
	α_L [L]	Longitudinal dispersivity (x direction)
	α_T [L]	Transversal dispersivity (y direction)
	α_V [L]	Vertical dispersivity (z direction)

**** Y_{i+1}=molar mass^i/molar mass^{i+1}. It is the ratio of the molar masses of the compounds in a degradation chain.***

2.4 Model IV. Unsaturated zone under an impervious area with zero infiltration

The conceptual model for Model IV is shown in Figure 7. Model IV simulates the water phase concentrations in the unsaturated zone overlying the unconfined aquifer with zero recharge using a vertical transport model, and then the concentrations in the aquifer using a horizontal transport model. The contaminant source is assumed to have a radius R_1 and a source concentration C_0. The source can be located below the terrain. The vertical transport model of Model IV simulates the water phase concentrations in the unsaturated zone between the contaminant source and to the top of the aquifer using a 2D steady-state analytical solution. The steady-state solution only considers 2D horizontal diffusive transport and thus concentration is not a function of the distance between the contaminant source and the top of the aquifer (i.e. concentration are constant in the vertical direction).

The vertical transport model simulates the concentration C_1 at the top of the aquifer which is then used as input to the horizontal model in order to simulate the concentrations downstream in the aquifer. The transfer of mass between the unsaturated zone and the saturated aquifer is assumed to occur by diffusion across the capillary fringe since the ground surface is impervious and there is no infiltration. The diffusive flux J across the capillary fringe is approximated by:

$$J(x,y) = -D_w^e \frac{C_1(x,y)}{B_f}$$

C1	CONCENTRATION IN THE WATER PHASE AT THE TOP OF THE AQUIFER (OUTPUT OF THE VERTICAL TRANSPORT MODEL)
Bf	DEPTH OF THE CAPILLARY FRINGE
D^e_w	EFFECTIVE DIFFUSION COEFFICIENT IN WATER (SEE EQUATION 8)

Equation 9

where $C_1(x,y)$ is the concentration at the bottom of the unsaturated zone, D^e_w is the effective diffusion coefficient of water and B_f is the capillary fringe thickness. The term $C_1(x,y)/B_f$ is an approximation of the diffusive concentration gradient assuming a small (zero) concentration in the saturated zone. The horizontal model then simulates the concentrations in the aquifer based on a 3D steady-state analytical solution including advection and dispersion in the aquifer. The horizontal model is a modified version of the horizontal model shown in Miljøstyrelsen (2016b). The following sections describe the vertical component of Model IV, the coupling between the vertical and the horizontal transport models, the horizontal model and the model parameters.

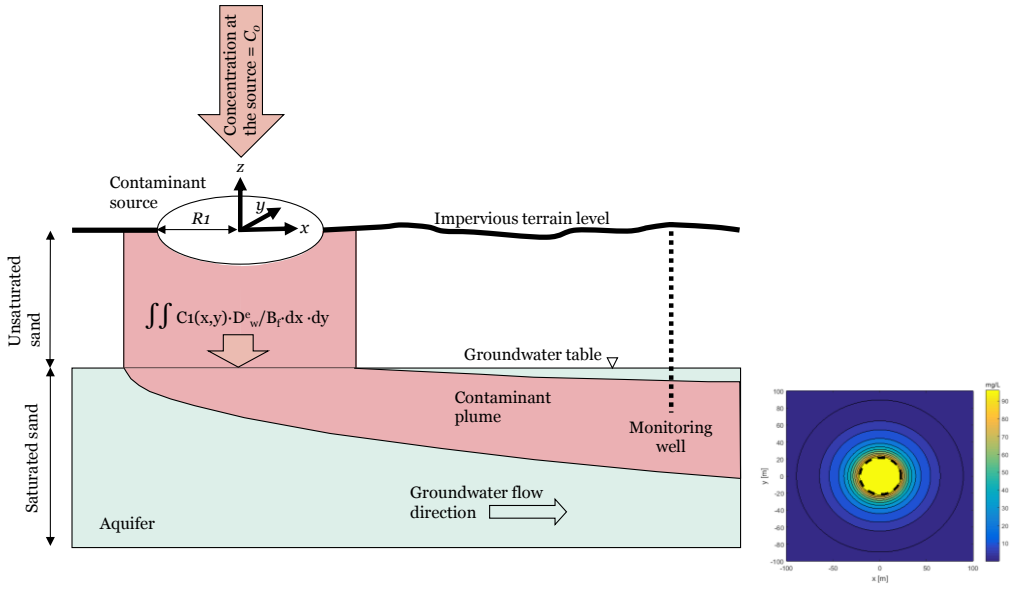

Figure 7. (Left) Conceptual model IV. Contaminant transport from a source located in the unsaturated zone and below an impervious area, downward to the top of the aquifer and then horizontal transport in the aquifer. (Right) Concentration at the top of the aquifer in plan view as a function of x and y; the black dashed line shows the location of the contaminant source (from the Mw Gjøes Vej model application).

2.4.1 Model IV. Unsaturated zone vertical transport model without infiltration

The vertical component of Model IV simulates the vertical contaminant transport in the water phase in the unsaturated zone when there is zero recharge, i.e. in the presence of an impervious area such as thick clays or paved areas. In this case the main mechanism of contaminant transport is gaseous diffusion in the horizontal direction.

Equation 10 the transport equation for volatile, reactive contaminants formulated in radial coordinates and in the case of zero recharge.

$$\frac{\partial(R\theta_w + K_H\theta_a)C_w}{\partial t} = (\theta_a K_H D_a^e + \theta_w D_w^e)\left(\frac{\partial^2 C_w}{\partial r^2} + \frac{1}{r}\frac{\partial C_w}{\partial r}\right) - \theta_w \lambda C_w$$

Cw	CONCENTRATION IN THE WATER PHASE
r	RADIAL DISTANCE FROM THE CENTER OF THE CONTAMINANT SOURCE
R	RETARDATION FACTOR
K_H	DIMENSIONLESS HENRY'S LAW CONSTANT
θw	WATER CONTENT
θa	AIR CONTENT
t	TIME
D^e_a	EFFECTIVE DIFFUSION COEFFICIENT IN AIR (SEE EQUATION 8)
D^e_w	EFFECTIVE DIFFUSION COEFFICIENT IN WATER (SEE EQUATION 8)
λ	FIRST ORDER DEGRADATION RATE

Equation 10

With the boundary conditions $C_w(0<r<R_1)=C_0$ and $C_w(r\rightarrow\infty)=0$, the steady-state solution was given by (Spiegel, 1968; Miljøstyrelsen, 2016a) and shown in Equation 11. Equation 11 is implemented in Model IV and it shows that the concentrations at steady-state are a function of the radial distance (and not the vertical distance in the *z* direction).

$$C_w(r) = \frac{C_0}{K_0(R_1\omega)} K_0(r\omega)$$

$$\omega = \sqrt{\frac{\theta_w \lambda}{\theta_a K_H D_a^e + \theta_w D_w^e}}$$

C_w	CONCENTRATION IN THE WATER PHASE
$K_0()$	MODIFIED BESSEL FUNCTION OF SECOND KIND AND ORDER 0
K_H	DIMENSIONLESS HENRY'S LAW CONSTANT
C0	SOURCE CONCENTRATION
R	RADIAL DISTANCE FROM THE CENTER OF THE CONTAMINANT SOURCE
R1	RADIUS OF THE CONTAMINANT SOURCE
θw	WATER CONTENT
θa	AIR CONTENT
D^e_a	EFFECTIVE DIFFUSION COEFFICIENT IN AIR (SEE EQUATION 8)
D^e_w	EFFECTIVE DIFFUSION COEFFICIENT IN WATER (SEE EQUATION 8)
λ	FIRST ORDER DEGRADATION RATE

Equation 11

2.4.2 Model IV. Coupling between the horizontal and vertical model

The conceptual model describing the coupling between the vertical and the horizontal transport model is shown in Figure 7. The vertical transport model simulates steady-state concentration $C_1(x,y)$ (Equation 11) at the top of the aquifer. The concentration at the top of the aquifer $C_1(x,y)$ is integrated over *x* and *y* and multiplied by the effective diffusion coefficient of water D^e_w and divided by the capillary fringe in B_f order to obtain the contaminant flux.

The steady-state solution (Equation 12) for the horizontal transport model is derived from Miljøstyrelsen, 2016b. Equation 12 is similar to the solution of Miljøstyrelsen (2016b) but with 2 changes (similar to Model III): (1) the mass discharge [M/L^2/T] from a point source at the top of the aquifer is now described by the function *J(x',y')*; (2) the integrals are calculated from -∞ to +∞ because the contaminated area at the top of the aquifer is now larger than the original source area.

The integrals are calculated numerically over a finite integration interval. The integration interval are set from *–150R1* +to *150R1*. The integration interval selected based on a different scenarios applied to the case study of MW Gjøes Vej (see Section 3.4.1). This selected integration interval is assumed to be appropriate for other cases.

$$c(x,y,z) = c_o + \int_{-\infty}^{\infty}\int_{-\infty}^{\infty} \frac{J(r)}{4\pi n\gamma\sqrt{D_y D_z}} \exp\left(\frac{u(x-x')}{2D_x} - \frac{\beta\gamma}{2D_x}\right) dx'\,dy'$$

$$J(r) = \frac{C_w(r) D_w^e}{B_f}$$

$$r = \sqrt{x'^2 \cdot y'^2}$$

$$\beta = \left(u^2 + 4D_x\lambda\right)^{1/2}$$

$$\gamma^2 = (x-x')^2 + \frac{D_x}{D_y}(y-y')^2 + \frac{D_x}{D_z}z^2$$

$$D_x = \alpha_L u$$

$$D_y = \alpha_T u$$

$$D_z = \alpha_V u$$

Cw	WATER PHASE CONCENTRATION CALCULATED USING EQUATION 11
Co	BACKGROUND CONCENTRATION
Bf	DEPTH OF THE CAPILLARY FRINGE
I	RECHARGE
n	POROSITY
Dx	DISPERSION COEFFICIENT IN THE X DIRECTION (LONGITUDINAL)
Dy	DISPERSION COEFFICIENT IN THE Y DIRECTION (TRANSVERSAL)
Dz	DISPERSION COEFFICIENT IN THE Z DIRECTION (TRANSVERSAL)
α_T	TRANSVERSAL DISPERSIVITY IN THE WATER PHASE
α_L	LONGITUDINAL DISPERSIVITY IN THE WATER PHASE
α_T	TRANSVERSAL DISPERSIVITY IN THE WATER PHASE
λ	FIRST ORDER DEGRADATION RATE
u	GROUNDWATER VELOCITY IN THE X DIRECTION

Equation 12

2.4.3 Model IV. Model parameters and output

Table 6 shows the user input model parameters for Model IV. The input parameters and variables in the tables are divided into three categories: Global parameters, Vertical model and Horizontal Model. The Model IV output is the contaminant concentration at a single or multiple user specified points x, y, z.

Table 6. User input parameters of model IV

	Input parameter	Description
Global parameters	Y_i [-]	Stoichiometric ratio of each compound i of the degradation chain
	I [L/T]	Recharge
	R_1 [L]	Radius of the source
Vertical model	$C_{0\ v}$ [M/L^3]	Concentration
	$k_{\_v}$ [T^{-1}]	First order degradation rate
	$n_{\_v}$ [-]	Porosity = water content
	$\theta_{w\ v}$ [-]	Water content
	$\alpha_{L\ v}$ [L]	Longitudinal dispersivity (z direction)
	$\alpha_{T\ v}$ [L]	Transversal dispersivity (z direction)
	$D_{a\ v}$ [L^2/T]	Free diffusion coefficient of air
	K_H [-]	Dimensionless Henry's law constant
	$foc_{\_v}$ [-]	Fraction of organic carbon
	K_{oc_v} [-]	Octanol-water partitioning coefficient
Horizontal model	H [L]	Thickness of the aquifer
	u [L/T]	Groundwater velocity
	k [T^{-1}]	First order degradation rate
	n [-]	Porosity
	α_L [L]	Longitudinal dispersivity (x direction)
	α_T [L]	Transversal dispersivity (y direction)
	α_V [L]	Vertical dispersivity (z direction)

**** Y_{i+1}=molar mass^{i}/molar mass^{i+1}. It is the ratio of the molar masses of the compounds in a degradation chain.***

2.5 Model V. Direct input from the contaminant source to the groundwater aquifer

The conceptual model for Model V is shown in Figure 8. Model V simulates the water phase concentrations in the aquifer using a horizontal transport model but with no vertical transport processes. The contaminant source is represented by the length L_x, the width L_y and the source concentration C_0. The source is located at the top of the aquifer. The horizontal model simulates the concentrations in the aquifer based on a 3D steady-state analytical solution that includes advection and dispersion in the aquifer.

Model V is the same as the model described in Miljøstyrelsen (2016b). In this model the vertical transport processes are not included since the source is assumed to be located at the top of the aquifer.

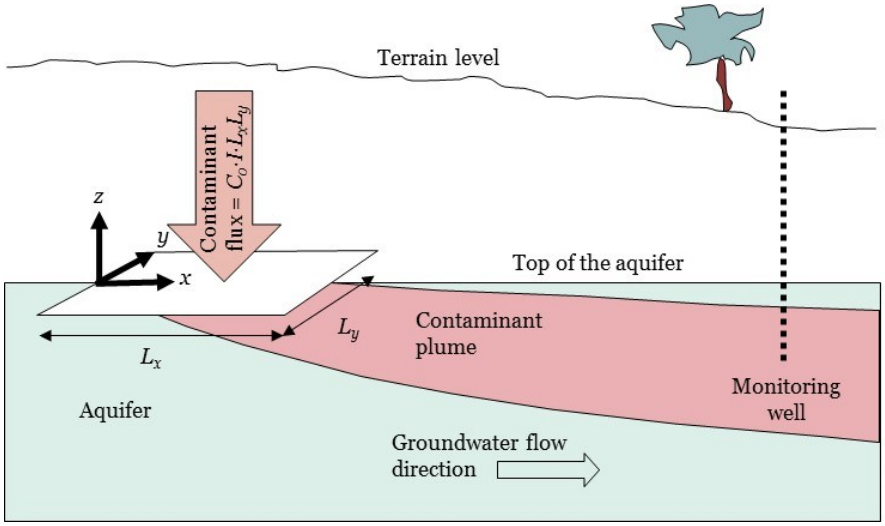

Figure 8. Conceptual model V. Horizontal contaminant transport from a source, located at the top of the aquifer. (this models is the same as Miljøstyrelsen, 2016B).

2.6 Incorporation of reactive decay chains

Reactive processes can be included in all five models in a similar way. In this section we only report the equations used in the model, however Miljøstyrelsen (2016b) provides the details of the approach.

Contaminant transport with reactive decay chains is described by Equation 13. In Equation 13, *R* and *D* have the same value for all the components *i*.

$$R\frac{\partial c_i}{\partial t} + \nabla c_i - \nabla\left(D\nabla c_i\right) = X\left(c_i\right)$$

$$X\left(c_i\right) = \begin{cases} -k_i c_i & i = 1 \\ y_i k_{i-1} c_{i-1} - k_i c_i & i = 2,3,...,n \end{cases}$$

R	RETARDATION FACTOR
Ci	CONCENTRATION OF THE ITH COMPOUND
t	TIME
D	HYDRODYNAMIC DISPERSION COEFFICIENT IN WATER
ki	FIRST ORDER DEGRADATION RATE OF THE ITH COMPOUND
yi	STOICHIOMETRIC RATIO OF THE ITH COMPOUND

Equation 13

We employ the method of Sun et al. (1999a; 1999b). That is, we define a set of auxiliary concentration variables:

$$a_i = \begin{cases} c_i & i = 1 \\ c_i + \sum_{j=1}^{i-1}\left(\prod_{l=j}^{i-1}\frac{y_{l+1}k_l}{k_l - k_i}\right)c_j & i = 2,3,....,n \end{cases}$$

The contaminant transport Equation 13 is then solved by the methods described for each of the models I-V with a_i replacing c_i. The solution for the components c_i is then obtained from a_i using:

$$c_i = \begin{cases} a_i & i = 1 \\ a_i - \sum_{j=1}^{i-1}\left(\prod_{l=j}^{i-1}\frac{y_{l+1}k_l}{k_l - k_i}\right)c_j & i = 2,3,....,n \end{cases}$$

3. Model applications

In this chapter several examples are presented showing how the models perform when applied to contaminated sites in Denmark. Each example includes a brief description of a contaminated site, shows how the model parameters were selected and presents the results. The modeling of the contaminant transport at the contaminated sites is based on historical data, so the observed contamination in the aquifer can be very different because the case may not consider results of recent investigations and remedial actions. Comparison of the model results with observation data was beyond the scope of this project. Note also that several simplifying assumptions are made in each case so that they can be described by the model.

The computational time depends on the model. Model I, II, and V have computational time of approximately 0-2 seconds for each simulated compound at a single point in the aquifer. Model III and IV have computational time up to 5 minutes for each simulated compound at a single point in the aquifer (this is because the numerical iterative convergence of the double integrals of Model III and IV is computationally demanding). This means that if we need to extract a concentration profile in the aquifer with 10 points, Model III and IV can take up to 50 minutes for each simulated compound. It may be possible to improve the computational time of Model III and IV by optimizing the integration routines (used to solve the integrals of Equation 8 and 12) and by exploiting geometrical symmetries of the model, however this was not attempted.

3.1 Rugårdsvej. Application of Model I

Rugårdsvej in Odense is contaminated with DCE and VC. Machinery was manufactured at the site in the period 1951-1989. Part of the area is now covered with asphalt. The source area is about 30 m long and 10 m wide. The contaminant mass discharging through the source (assuming 300 mm/y infiltration according to JAGG 2.0) is 33 kg/y of DCE and 0.63 kg/y of VC. In the simulation degradation of both components is assumed to occur.

3.1.1 Geology and hydrogeology

The primary aquifer is comprised of meltwater sand and gravel and is overlain by a 25-30 m clay till. Locally there is a 1 m thick upper aquifer of fine-medium graded meltwater sand. The secondary aquifer is about 12 m.b.s. and is overlain by fill and clay till with sand, silt and clay lenses. Figure 9 shows the geological profile in the area of Rugårdsvej.

The water table in the secondary aquifer is located about 3-4 m.b.s. The clay layers are assumed not to be fractured. JAGG 2.0 provides a recharge of 300 mm/y; Jørgensen et al. (2007b) proposed a recharge of 100 mm/y and Miljøstyrelsen (2011) reported a recharge of 8 mm/y at the site.

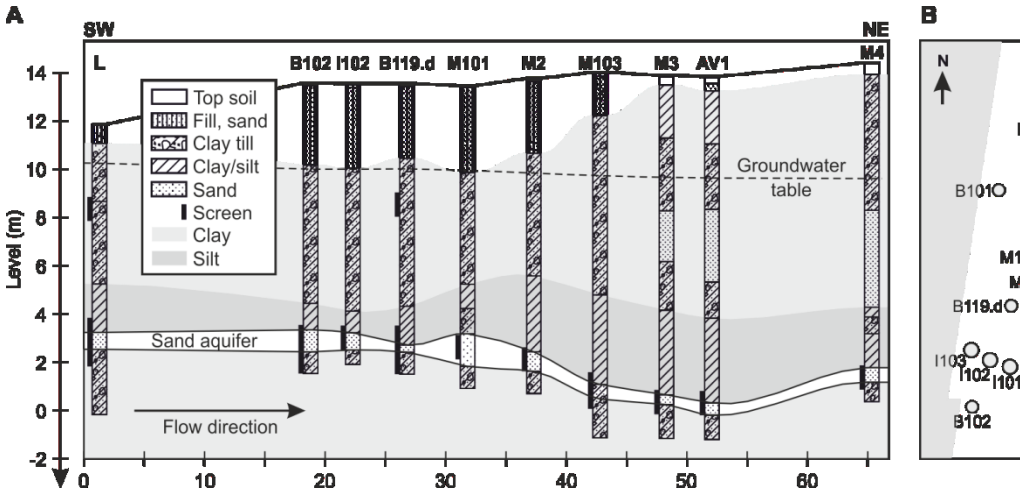

Figure 9. (A) Geological profile at Rugårdsvej 234-238 i Odense; (B) Plan view of the site (Scheutz et al., 2008).

3.1.2 Contamination at the site

At Rugårdsvej 95% of the overall contaminant load from the source consists of DCE (Jørgensen et al., 2007a). The original contaminant spill was TCE; however it has degraded into DCE and VC which were found to be the main contaminants at the site.

The vertical and horizontal spreading of contaminants is shown in Figure 10. The source is estimated to be 4-9 m.b.s. and the total concentration of chlorinated solvent in the source is approximately 10 mg/kg of dry soil (Jørgensen et al. 2007a).

The highest concentration of DCE in the source zone is 371 mg/l (77 mg/kg of dry soil), and 7 mg/l VC (1.9 mg/kg of dry soil) was measured at the borehole M1 (Figure 9) at 4-5 m.b.s. (Jørgensen et al. 2007). There are iron reducing conditions in and around the contaminant source, with a trend to less reduced conditions with increasing distance from the source (Jørgensen et al., 2007a).

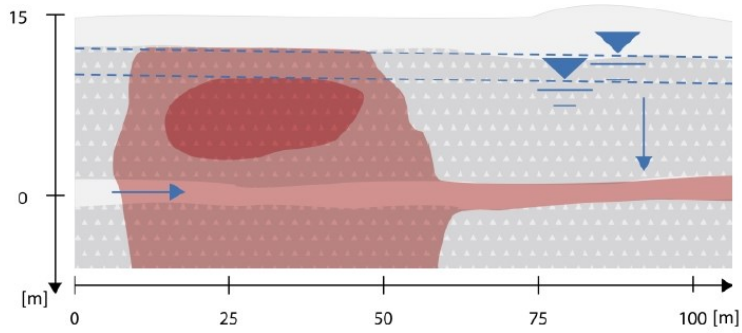

Figure 10. Cross Section of the contaminant plume at Rugårdsvej (Jørgensen et al., 2003).

3.1.3 Conceptual model and parameters for Rugårdsvej

Model I was chosen because the vertical transport processes from the source to the top of the sand aquifer (Figure 9 and 10) take place in the saturated homogenous clay. The vertical contaminant transport of DCE and VC was simulated from the point where the highest concentrations were measured to the top of the upper aquifer (the vertical distance between the source and the upper aquifer was estimated to be approximately 6 m). The source concentrations of DCE and VC are assumed to be equal to the highest measured concentrations to ensure a conservative risk estimate in line with the recommendations in JAGG. The length and width of

the source area were assumed to be the same as estimated in Miljøstyrelsen (2016b). Table 7 summarizes all the model parameters used. The model was run for the 3 different recharge values as shown in Table 7.

Table 7. Model I parameters used for Rugårdsvej.

	Parameter	Description	Value	Source
Global parameters	Y	Stoichiometric ratio VC- DCE	0.648*	
	I	Recharge	*300 mm/y* *100 mm/y* *8** mm/y*	JAGG 2.0 Jørgensen et al. (2007b) Miljøstyrelsen (2011)
	L_x	Source length	*30 m*	Jørgensen et al. (2007a)
	L_y	Source width	*10 m*	Jørgensen et al. (2007a)
Vertical model	C_{0_v}	Concentration of DCE	*371 mg/L*	Jørgensen et al. (2007a)
		Concentration of VC	*7 mg/L*	Jørgensen et al. (2007a)
	$k_{\_v}$	First order degradation rate of DCE	*0.0001 day^{-1}*	JAGG 2.0
		First order degradation rate of VC	*0.0004 day^{-1}*	JAGG 2.0
	$n_{\_v}$	Porosity = water content	*0.35*	JAGG 2.0
	α_{L_v}	Longitudinal dispersivity (z direction)	*0.014*	JAGG 2.0
	$Z_{\_v}$	Distance between the bottom of the source and the top of the aquifer	*6 m*	
	D_{w_v}	Free diffusion coefficient in water	$7.17 \cdot 10^{-10}$ m^2/sec	JAGG 2.0
Horizontal model	H	Thickness of the aquifer	*1 m*	Miljøstyrelsen, 2016b
	u	Groundwater velocity	*126 m/y*	Miljøstyrelsen, 2016b
	k	First order degradation rate of DCE	*0.0001 day^{-1}*	Miljøstyrelsen, 2016b
		First order degradation rate of VC	*0.0004 day^{-1}*	Miljøstyrelsen, 2016b
	n	Porosity	*0.25*	Miljøstyrelsen, 2016b
	α_L	Longitudinal dispersivity (x direction)	*1 m*	Miljøstyrelsen, 2016b
	α_T	Transversal dispersivity (y direction)	*0.01 m*	Miljøstyrelsen, 2016b
	α_V	Vertical dispersivity (z direction)	*0.005 m*	Miljøstyrelsen, 2016b

* ratio of VC and DCE molar mass = 62.5 [g/mol]/96.94 [g/mol]
** found by multiplying the vertical head gradient (0.05) by the hydraulic conductivity ($5 \cdot 10^{-9}$ m/s)

3.1.4 Results for Rugårdsvej

Figure 11 shows the contaminant distribution simulated by vertical model I from the source to the top of the aquifer (6 m) at Rugårdsvej. The results are shown for the three different recharge rates. Model I was chosen because the vertical transport processes from the source to the top of the sand aquifer (Figure 11) take place in the saturated homogenous clay. The vertical contaminant transport of DCE and VC was simulated from the point where the highest concentrations were measured to the top of the upper aquifer (the vertical distance between the source and the upper aquifer was estimated to be approximately 6 m). The source concentrations of DCE and VC are assumed to be equal to the highest measured concentrations to ensure a conservative risk estimate in line with the recommendations in JAGG. The length and width of the source area were assumed to be the same as estimated in Miljøstyrelsen (2016b). Table 7 summarizes all the model parameters used. The model was run for the 3 different recharge values as shown in Table 7.

The results vary greatly depending on the different recharge rates, showing that the model is highly sensitive to the recharge input. Moreover, the variation of concentrations with the depth below the source shows that vertical transport processes significantly influence the concentrations reaching the aquifer. Generally, the larger the vertical distance between the source and the top of the aquifer, the greater the decrease in concentration. However, in the case of degradation compounds, such as VC in this case, concentrations are shown to increase up to a certain depth below the source and then decrease. The increase of concentration of VC is due to the degradation of DCE into VC during the vertical transport from the source to the aquifer. If the degradation rates are zero (for the vertical model) then concentrations are not reduced in the vertical model.

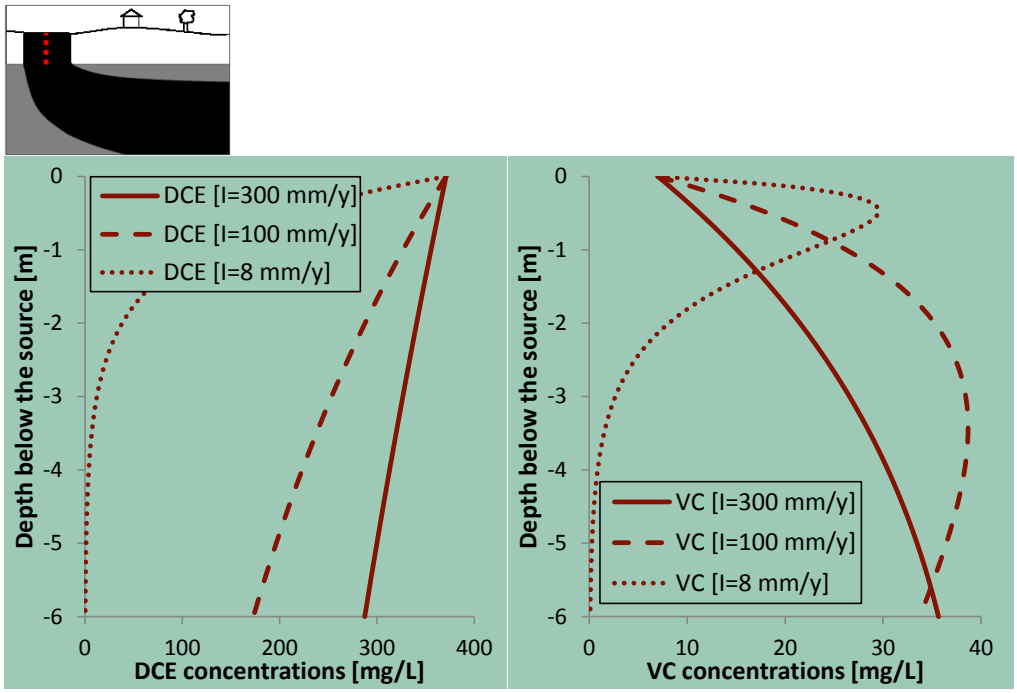

Figure 11. concentration of DCE (left) and VC (right) as a function of the depth below the source and the different recharge rates I. the level -6 M corresponds to the top of the upper aquifer.

The output concentration at the end of the vertical model downward pathway (the top of the aquifer) is used as input to the horizontal transport model. For instance the DCE concentration at the end of the vertical transport pathway (depth below the source is -6 m. See Figure 11) is 289 mg/L for a recharge rate of 300 mm/y. This concentration is multiplied by the contaminant

source area $L_x \cdot L_y$ and the recharge I rate in order to obtain the input mass discharge for the horizontal model.

Figure 12 shows the concentrations of DCE and VC as a function of distance x in the aquifer ($y=0$) up to 100 m downstream of the source. Two solutions are presented, the first one uses Model I and the second one uses Model I excluding the vertical transport model (this means that the input source concentrations of DCE and VC are directly applied to the horizontal model, i.e. Model V is used). The concentrations do not vary in the z direction since the top of the aquifer is thin and so the 2D horizontal transport model (Miljøstyrelsen, 2016b) was used. The results show that including the vertical transport model reduces the output concentrations of DCE and increases the output concentration of VC. This is because DCE degrades to VC during the vertical transport from the source to the top of the aquifer. A significant difference in concentrations 100 m downstream of the source (particularly the VC concentration) is observed if the vertical transport processes are included.

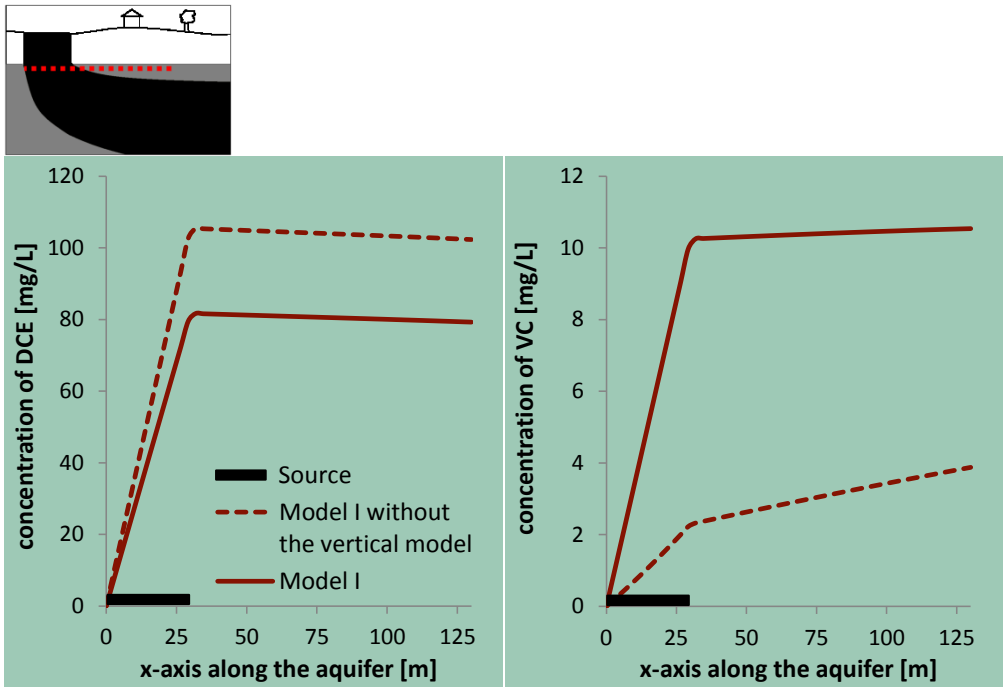

Figure 12. concentration of DCE (left) and VC (right) in the aquifer (note that there are fully mixed conditions in the thin aquifer so there is no variation in concentrations in the z direction). I=300 MM/Y.

3.1.5 Rugårdsvej example assuming contamination of benzene and toluene

This section shows the results of a hypothetical example applying Model I to a site similar to Rugårdsvej, but with the chlorinated solvents replaced by the more degradable compounds benzene and toluene. Results demonstrate how changes in degradation rates change contaminant concentrations entering the aquifer.

The input model parameters are still as shown in Table 7 but with the following few changes applied: (1) the input concentration of benzene and toluene are assumed to be $C_{0\_v}=50$ *mg/l*; (2) the free diffusion coefficient in water of benzene is $D_{w\_v}=9.3 \cdot 10^{-10}$ m^2/s and that of toluene is $D_{w\_v}=8.56 \cdot 10^{-10}$ m^2/s (JAGG 2.0); (3) the first order degradation rate of benzene is $k_{\_v}=0.001$ day^{-1} and for toluene is $k_{\_v}=0.01$ day^{-1} (JAGG 2.0), so about 10-100 times higher than for DCE and VC.

Figure 13 shows the results of the vertical transport model from the source to the top of the aquifer (6 m.b.s.) using Model I. The results show a significant reduction of concentration with increasing the depth below the source, particularly for toluene. The overall reduction of concentration is more pronounced compared to the results shown above in Figure 13 for DCE. This is because the first order degradation rates of toluene and benzene are much higher than DCE.

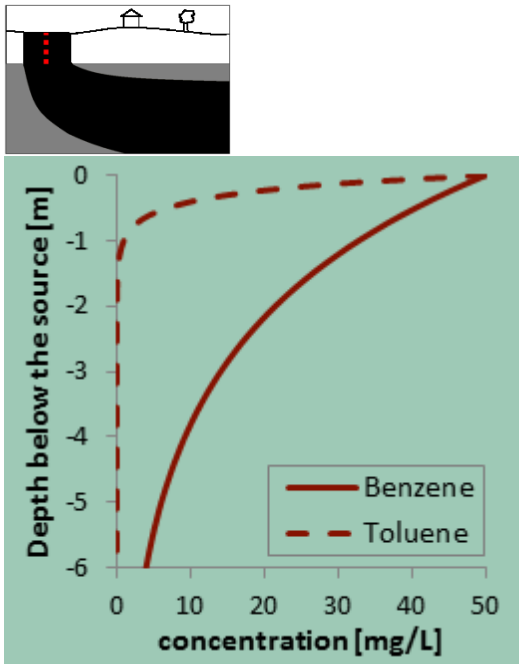

Figure 13. Model I application to high degradable compounds. concentration of benzene and toluene as a function of the depth below the source. An infiltration rate of 300 MM/Y was used and the level -6 M corresponds to the top of the aquifer.

Figure 14 shows the concentrations of benzene and toluene as a function of distance *x* in the aquifer (*y=0*) up to 100 m downstream the source. Two solutions are presented, the first one uses Model I and the second one uses Model I without the vertical transport processes (this means that the input source concentrations of benzene and toluene are directly applied to the horizontal model). The concentrations do not change in the *z* direction since the 2D solution (Miljøstyrelsen, 2016b) was used. The results show a significant reduction of concentration if the vertical transport processes are included.

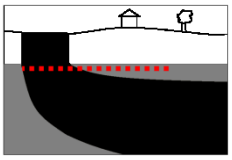

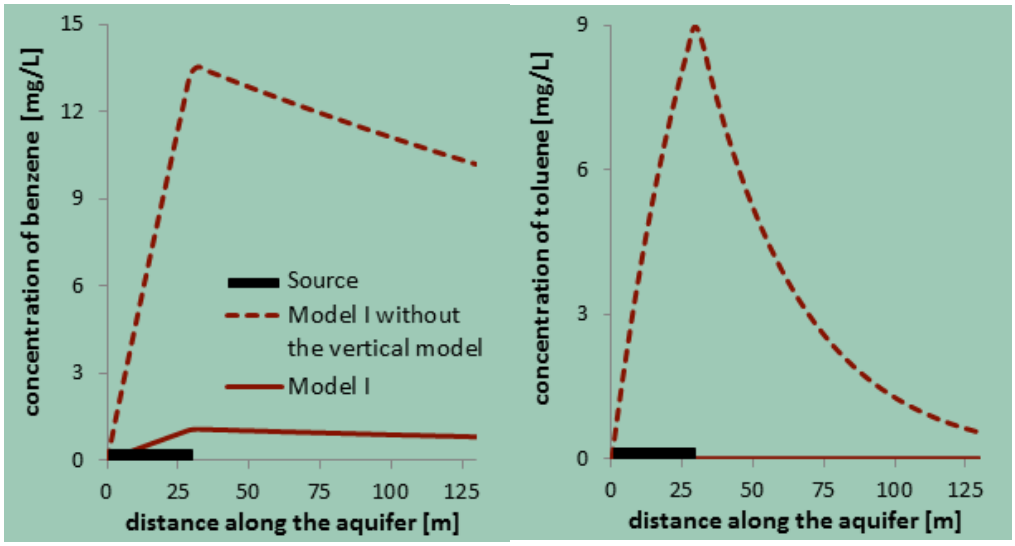

Figure 14. Concentration of benzene and toluene in the aquifer. The aquifer is thin and so is fully mixed in the vertical direction and so the 2d solution is used. I=300 MM/Y

3.1.6 Conclusion of Model I application

The results of the Model I application to Rugårdsvej showed the following:

- There is a significant difference in the predicted concentrations of DCE and VC in the aquifer 100 m downstream of the source if the vertical transport processes are included in the model.
- The vertical transport processes are more pronounced for more degradable contaminants.
- Model results are very dependent on the recharge rate. The greater the recharge, the larger the pore water velocity, and the lower the degradation.

3.2 Vadsbyvej. Application of model II

Vasbyvej in Taastrup is contaminated with PCE, TCE, DCE and VC. Several contaminant source areas were identified (Miljøstyrelsen, 2009b). Only one of the source areas was modeled in this report. The source area considered is 10 m long and 5.5 m wide and consists of PCE. The contaminant mass discharge leaving the 55 m^2 source area is 2.6 kg/y (assuming 82 mm/y recharge according to Miljøstyrelsen (2009b)). The contaminants are degradable and the sequential degradation processes are included in the model, where PCE is degraded to TCE and DCE. Only the results for PCE are shown here, but the model can simulate the whole decay chain.

3.2.1 Geology and hydrogeology

The local geology in the area is shown in Figure 15. At the site there is an upper sandy aquifer of 2.4 m thickness overlain by 15 m of clayey till with fractures. The estimated bulk hydraulic conductivity of the clayey till is $1.3 \cdot 10^{-8}$ m/s and the vertical head gradient in the clayey till is 0.2 (Miljøstyrelsen, 2009b). This gives a recharge of 82 mm/y. The hydraulic conductivity of the upper sandy aquifer is $3 \cdot 10^{-5}$ m/s and the horizontal head gradient is 0.0007 (Miljøstyrelsen, 2009b). This results in a horizontal velocity of 3.3 m/y (using a porosity of 0.2 as in Miljøstyrelsen (2009b)). The fracture spacing at the bottom of the caly till shown in Figure 15 (approximately 15 m.b.s.) was estimated to be 5.6 m (Miljøstyrelsen, 2009b).

3.2.2 Contamination at the site

Figure 15 shows the location of the contaminant source areas as presented by Miljøstyrelsen (2009b). In this example we selected the area 'Zone A2-SZ' to be used in our Model II application. The concentration of PCE is 58 mg/L and the source area is 55 m^2. The source length was estimated from the figure to be 10 m and the width was derived from the area and the source length (5.5m=55m^2/10m). The distance from the source to the top of the groundwater is estimated to be 7 m. There are anaerobic conditions, so chlorinated solvent degradation is expected to occur.

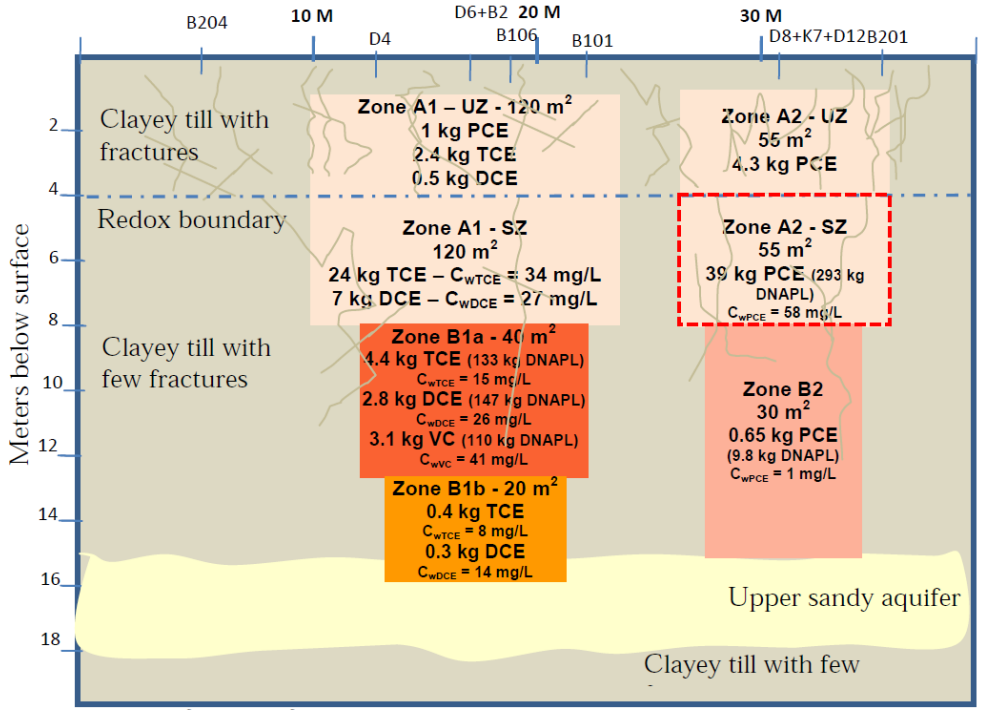

Figure 15. Conceptual model of contaminant source distribution and average aqueous concentrations at vadsbyvej (disregarding the DNAPL phase) (Miljøstyrelsen, 2009B). the source enclosed by the red dashed line is modelled.

3.2.3 Conceptual model and parameters for Vadsbyvej

Model II was chosen because the vertical transport processes from the source to the top of the aquifer occur in a saturated fractured clay overlying the aquifer. Table 8 summarizes all the model parameters used in Model II. The model was run for the 2 different recharge rates as shown in Table 8.

Table 8. Model II parameters used for Vadsbyvej

	Input parameter	Description	Value	Source
Global parameters	I	Recharge	*250 mm/y* *82 mm/y*	JAGG 2.0 Miljøstyrelsen (2009b)
	L_x	Source length	*10 m*	Estimated from Figure 15
	L_y	Source width	*5.5 m*	Estimated from Figure 15
Vertical model	C_{0_v}	Concentration of PCE	*58 mg/L*	Miljøstyrelsen (2009b)
	$k_{\_v}$	First order degradation rate of PCE	*0.0005 day^{-1}*	JAGG 2.0
	$n_{\_v}$	Porosity = water content	*0.3*	Miljøstyrelsen (2009b)
	α_{L_v}	Longitudinal dispersivity (z direction)	*0.1 m*	Miljøstyrelsen (2009b)
	$Z_{\_v}$	Distance between the bottom of the source and the top of the aquifer	*7 m*	Estimated from Figure 15
	D_{w_v}	Free diffusion coefficient in water PCE	5.71·10^{-10} m^2/sec	Miljøstyrelsen (2009b)
	$2B_{\_v}$	Fracture spacing at the bottom of the clay till	5.6	Miljøstyrelsen (2009b)
	$kb_{\_v}$	Bulk hydraulic conductivity	1.3·10^{-8} m/sec	Miljøstyrelsen (2009b)
	K_d**	Sorption coefficient	1.65 L/kg	Lu et al. (2011)
Horizontal model	H	Thickness of the aquifer	*2.4 m*	Miljøstyrelsen (2009b)
	u	Groundwater velocity	*3.3 m/y**	
	k	First order degradation rate of PCE	*0.0005 day^{-1}*	JAGG 2.0
	n	Porosity	*0.2*	Miljøstyrelsen (2009b)
	α_L	Longitudinal dispersivity (x direction)	*1 m*	Miljøstyrelsen (2016b)
	α_T	Transversal dispersivity (y direction)	*0.01 m*	Miljøstyrelsen (2016b)
	α_V	Vertical dispersivity (z direction)	*0.005 m*	Miljøstyrelsen (2016b)

** found by multiplying the horizontal head gradient (0.0007) with the hydraulic conductivity (3·10^{-5} m/s) and dividing by the porosity (0.2). Values obtained from Miljøstyrelsen (2009b).*
*** Kd values specific for clayey tills can be found in Lu et al. (2011)*

3.2.4 Results for Vadsbyvej

Figure 16 (left) shows the PCE concentration between the source and the top of the aquifer (degradation of PCE to TCE and DCE was simulated, but only the results for PCE are shown). Results for the two different recharge rates *I* of Table 8 are shown. Overall, the longer the percolation time from the source to the top of the aquifer, the greater the impact of degradation during vertical transport and the higher the reduction in the concentrations reaching the aquifer. The percolation time from the source to the top of the aquifer depends on the recharge *I*, fracture spacing *2B,* and bulk hydraulic conductivity K_b. When the degradation rates are zero (vertical model) then the vertical model does not produce variations in the steady-state concentrations. The reduction in concentration from the source to the top of the aquifer is approximately 25% when the recharge is *I*=82 mm/y, while it is only 8% when the recharge rate is 250 mm/yr.

One assumption made in all the models is that of steady-state. It is important to check the validity of this assumption. Figure 16 (right) shows the PCE concentration as a function of time simulated using the model DTU v1D (Chambon et al., 2011). The results show that it takes approximately 20 years for a recharge of 250 mm/y, and 50 years for a recharge of 82 mm/y to reach steady-state concentrations. The steady-state solution provides a conservative risk assessment because transient concentrations are lower than those determined by the steady-state solution. Since almost steady-state concentrations are obtained after 20 years it is acceptable to neglect temporal changes in the concentration at the site.

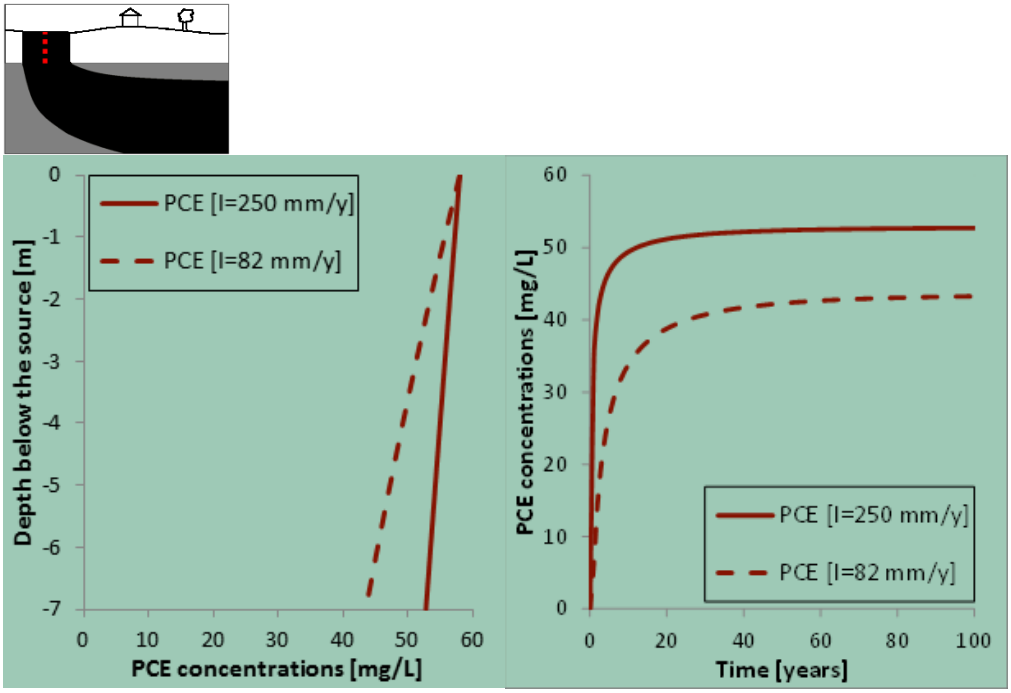

Figure 16. Concentration of PCE as a function of the depth below the source and the different recharge rates I. (left). the level -7 M corresponds to the top of the aquifer. Concentration of PCE as a function of time (using the model DTU v1d of Chambon et al., 2011) at 7m depth (right).

The output concentration at the end of the vertical model downward pathway (the top of the aquifer) is used as input to the horizontal transport model. For instance the PCE concentration at the end of the vertical transport pathway (depth below the source -7 m. See Figure 16) is 53 mg/L for a recharge rate of 250 mm/y. This concentration is multiplied by the contaminant source area $L_x \cdot L_y$ and the recharge *I* rate in order to obtain the input mass discharge for the horizontal model.

Figure 17 shows the concentrations of PCE as a function of distance *x* in the aquifer (*y=0*) up to 100 m downstream of the source. Two solutions are presented; the first one uses Model II and the second one uses Model II without the vertical transport model (this means that the input source concentrations of PCE are directly applied to the horizontal model, i.e. Model V). Because the aquifer is thin, the 2D horizontal model (Miljøstyrelsen, 2016b) was used and the estimated concentrations in the aquifer do therefore not vary in the z direction. The results show that including the vertical transport model reduces the output concentrations of PCE. However, the difference in PCE concentration predicted by the two models at 100 m downstream of the source is very small. This is because the groundwater velocity in the aquifer is very low (*u=3.3 m/y*) so that the residence time in the aquifer is very long, allowing for significant degradation to occur before reaching a point 100 m downstream the source.

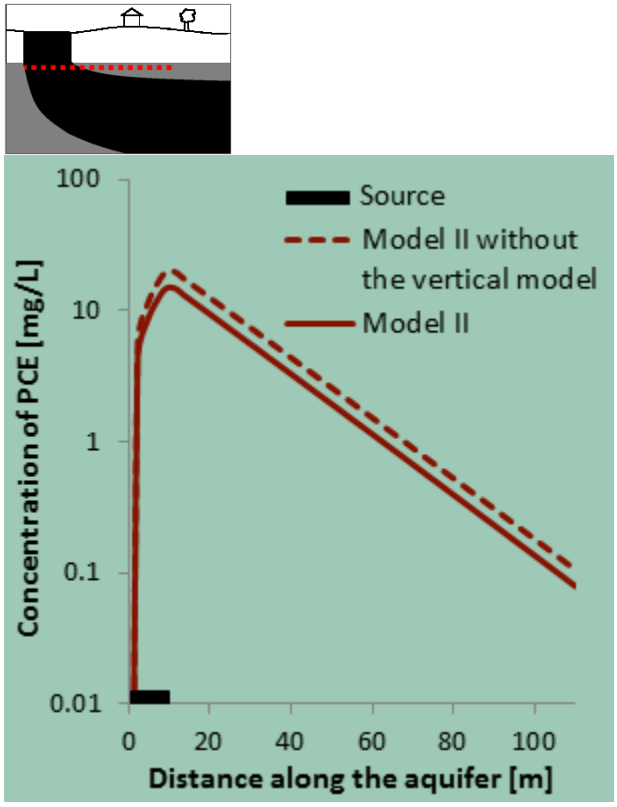

Figure 17. Concentration of PCE in the aquifer (there are fully mixed conditions in the aquifer, a 2d solution is used so there is no variation in concentrations in the z direction). I=82 MM/Y. Note that concentrations along y-axis are log-scale.

3.2.5 The effect of the fracture spacing parameter 2B

The model input parameter fracture spacing 2B is difficult to estimate and Christiansen et al. (2006), Videncenter for Jordforurening (2008), and Klint et al. (2013) showed that the fracture spacing in Danish clayey tills can vary between 0 and 5 m in the top 8 m.b.s, and that the fracture spacing increases with the depth below the surface. Figure 18 shows the PCE concentrations from Model II as a function of the depth below the source and for different fracture spacing *2B* (when the fracture spacing, recharge rates and bulk hydraulic conductivity are specified, the model calculates the resulting vertical gradient and fracture aperture using Equation 5). The results show that the smaller the fracture spacing, the higher the reduction in PCE concentrations. This is because a smaller fracture spacing reduces the percolation time of contaminants from the source to the top of the aquifer (the same amount of infiltration is spread over a larger number of fractures that are now closer to each-other).

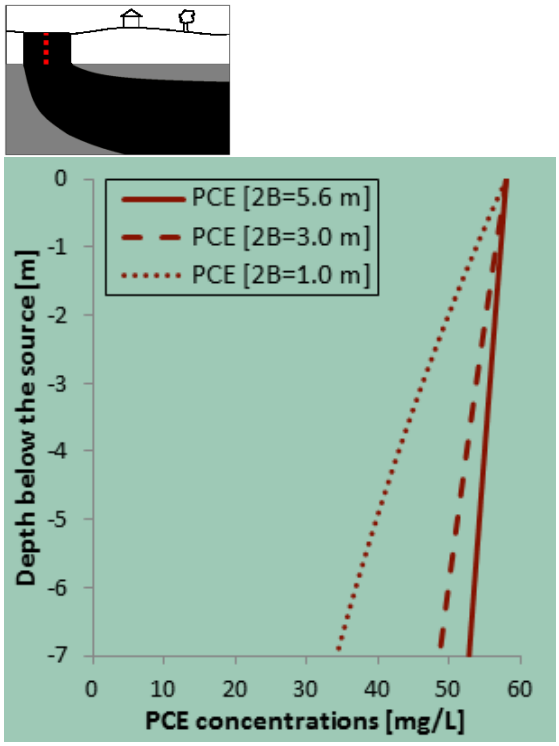

Figure 18. Concentration as a function of the depth below the source and different fracture spacing 2b. the recharge rate is I=250 MM/Y.

3.2.6 The assumption of fully mixed conditions at the bottom of the fractured aquitard

The fracture transport Model II assumes that the contaminant output from the fractures is fully mixed over the whole source area at the top of the aquifer. This section investigates the validity of this assumption.

To test the fully mixed assumption, a coupled COMSOL Multiphysics model was used to run various scenarios where the contaminant flux from the fractured clay is mixed at the top of the aquifer in different ways. Each scenario simulates the contaminant concentration in the aquifer based on different fracture distributions.

The scenarios are illustrated in Figure 19 and are:

1. Matlab, fully mixed. The concentrations in the aquifer are simulated using the horizontal Model II. The contaminant mass discharge is uniform over the source area.
2. Multiphysics, fully mixed. The concentrations in the aquifer are simulated using Multiphysics with a uniform mass discharge over the source area.
3. Multiphysics, perpendicular fractures. The source is modelled with 2 line sources having a specified contaminant flux per unit length and with a distance of 2B=5.6m. The line source is perpendicular to the flow direction in the aquifer (aligned with the y axes of Model II).
4. Multiphysics, angled fractures. The source is modelled as a line source having a specified contaminant flux per unit length. The line source is oriented with an angle of 30 degrees compared to the flow direction in the aquifer.
5. Multiphysics, longitudinal fracture. The source is modelled as a line source having a specified contaminant flux per unit length. The line source is oriented in the flow direction in the aquifer (aligned with the x axes of Model II).
6. Multiphysics, longitudinal parallel fracture. The source is modelled as a line source having a specified contaminant flux per unit length. The line source is oriented in the flow direction in the aquifer (aligned with the x axes of Model II).

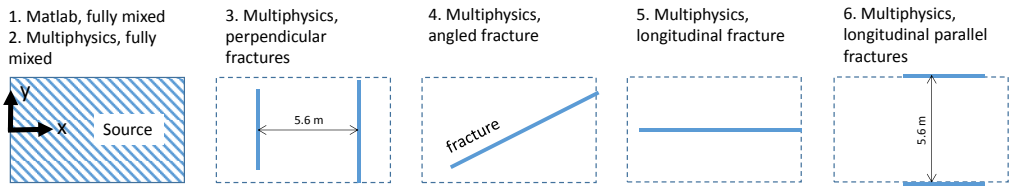

Figure 19. Representation of the scenarios. the source and fractures are shown on a plane corresponding the top of the aquifer (the x direction is the groundwater flow direction). The total length of the fractures in each scenarion is the same in order to have the same contaminant mass discharge in all scenarios.

Each scenarios has the same contaminant mass discharge to the aquifer. The total mass discharge assuming fully mixed conditions is 0.73 kg/y (given by $I \cdot L_x \cdot L_y \cdot C$ = *250 mm/y·10 m·5.5 m·52.8 mg/L*). The discharge per unit length of fractures is 0.074 kg/y/m (*given by* $2b \cdot v_f C$ = $4.9 \cdot 10^{-5}$ *m·29000 m/s·52.8 mg/L*). Thus, a 9.8 m long fracture gives a mass discharge of 0.73 kg/y (the fracture length was found by: *9.8 m=0.73 kg/y / 0.074 kg/y/m*). The model parameters of Vadsbyvej (Table 8) are used, apart from the aquifer thickness which was set to be 12 m and the groundwater velocity which was set to be 33 m/y, allowing an easier comparison of the results between the Matlab and Multiphysics models.

Figure 20 (a) shows the concentration in the aquifer along the flow direction (x-axis of Model II) and at a depth of 0.01 m below the top of the aquifer. All scenarios have similar concentrations except for the scenarios 'Multiphysics, longitudinal fracture' which has much higher concentrations because the concentration is plotted right below the source fracture, and 'Multiphysics, longitudinal parallel fractures' which has much lower concentrations because the fractures are not aligned with the central line of the contaminant plume. Patterns are different close to the source area because of the different fracture layouts in the different scenarios. Figure 20 (b) shows the concentration in the aquifer at 4 m depth below the top of the aquifer and 100 m downstream the source. Figure 20 (c) shows the concentration in the aquifer 100 m downstream the source as a function of the depth below the top of the aquifer (z-axis) and at *y=0m*. All scenarios show similar patterns except for the 'Multiphysics, longitudinal parallel fractures'. The 'Matlab, fully mixed' model estimates concentrations greater than those of the Multiphysics scenarios except for the 'Multiphysics, longitudinal fractures' scenario.

Results show that the Matlab Model II with the assumption of fully mixed condition is reasonable, with concentrations being larger than the models explicitly simulating the fractures except for the scenario 'Multiphysics, longitudinal fractures' which is very unlikely to occur. Differences between the fully mixed and discrete fracture models are a little larger directly under the source (Figure 20 a) but diminish with distance downstream of the source due to dispersion effects.

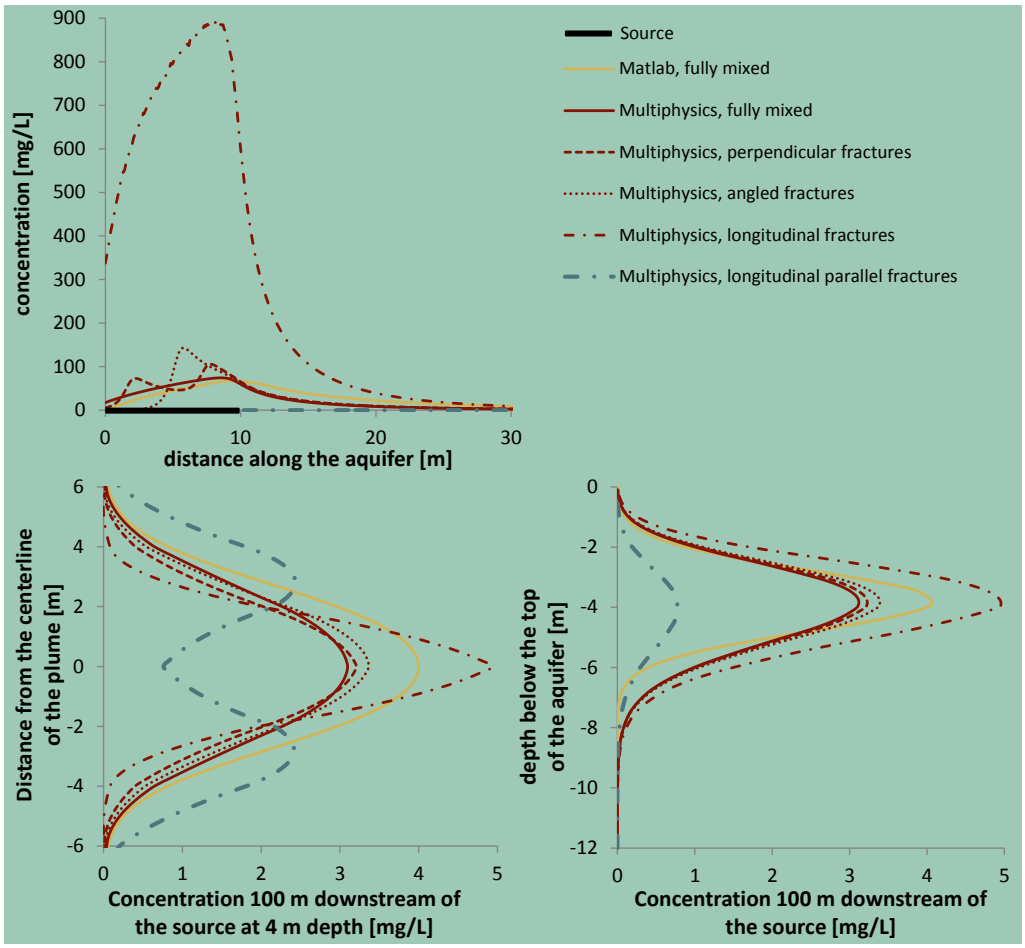

Figure 20. Concentration in the aquifer as a function of different fracture geometries. (A) concentrations along the x-axes and at 0.01 M DISTANCE FROM THE TOP OF THE AQUIFER. (B) concentrations as a function of the distance below the top of the aquifer 100 M downstream the source. (C) cONCENTRATIONS AS A FUNCTION OF distance from the centerline of the plume at a depth of 4 M below the top of the aquifer and 100 M DOWNSTREAM THE SOURCE.

3.2.7 Conclusion of Model II application

The results of the Model II application to Vadsbyvej showed the following:

- There is only a small difference in the concentration in the aquifer 100 m downstream the source if the vertical transport processes are included in the model. This is because the vertical transport process have little effect on the concentration from the source to the top of the aquifer.
- In the vertical transport model, degradation processes have little effect on the concentration from the source to the top of the aquifer because of the high velocity in the fractures.
- The recharge rate affects model results. The larger the recharge, the higher the pore water velocity, and the lower the degradation.
- The model is sensitive to fracture spacing *2B*. The larger the fracture spacing, the higher the water velocity in the fractures, and the lower the degradation.
- The assumption of fully mixed conditions (uniform concentration distribution) at the top of the aquifer was shown to be reasonable.

3.3 MW Gjøes Vej. Application of model III

At MW Gjøes Vej 8 in Reerslev a former dry-cleaning facility, operating in the period 1956-1977, has caused widespread contamination with PCE. It has been estimated that the amount of PCE and degradation products spilled at the site is between 3 and 10 tons with PCE comprising about 50% of the total weight (Niras, 2009).

3.3.1 Geology and hydrogeology

The local geology is shown in Figure 21. The top 7 m consists of unsaturated clayey till and then 20 m of meltwater sand and gravel. Only the lowest part of the sand is saturated. Below the sand and gravel layer there is a 1 m thick layer of clayey till that extends approximately 1500 m downstream of the contaminant source. Below the clayey till there is a 25 m deep regional limestone aquifer (Krüger, 2004).

The upper secondary aquifer is unconfined and the head level about 25 m.b.s. There is downward vertical advective flow in the clayey till layer that is assumed to equal the recharge rate.

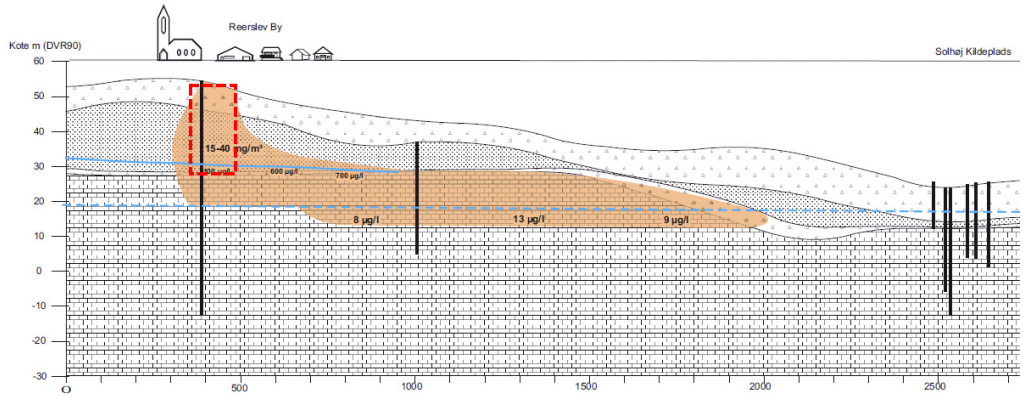

Figure 21. Geological and conceptual contaminant transport model at MW Gjøes Vej. The red dotted line shows approximately the area that is modelled. Modified from niras (2009).

3.3.2 Contamination at the site

There are two areas contaminated by chlorinated solvents exceeding the quality criteria of the Danish EPA (5 mg/kg) (Krüger, 2004; Miljøstyrelsen, 2014). The concentration that are used as input to Model III are greatest at 3.0-5.0 m.b.s. (Krüger, 2004). The areal extent of the contaminant source was assumed to be the same as that estimated in Miljøstyrelsen (2016b).

3.3.3 Conceptual model and parameters for MW Gløes Vej

Model III was selected because vertical transport from the source to the top of the aquifer occurs in an unsaturated sand and the recharge in the area is greater than zero. The vertical contaminant transport was simulated from the top of the sandy layer (assumed to be the bottom of the source) to the groundwater table (the red dotted line of Figure 21 shows the model area). The vertical distance between the bottom of the source zone (i.e. the the sand) and the top of the unconfined aquifer was estimated by Miljøstyrelsen (2011) to be approximately 18 m. The source concentrations are assumed to be equal to the highest measured concentrations. The length and width of the source area were assumed to be the same as estimated in Miljøstyrelsen (2016b). The horizontal model simulates the transport only in the uppermost secondary aquifer which is situated on top of a thin clayey till layer (27-29 m.b.s., Figure 21). Table 9 summarizes the model parameters used.

Table 9. Model III parameters used for MW Gjøes Vej.

	Input parameter	Description	Value	Source
Global parameters	Y	PCE – TCE (molar mass ratio) TCE –DCE (molar mass ratio) DCE –VC (molar mass ratio)	0.79 0.74 0.64	molar mass of each compound was obtained from JAGG 2.0
	I	Recharge	*250 mm/y*	JAGG 2.0
	L_x	Source length	*45 m*	Miljøstyrelsen, 2016b
	L_y	Source width	*30 m*	Miljøstyrelsen, 2016b
Vertical model	C_{0_v}	Concentration of PCE	*97 mg/L*	Miljøstyrelsen, 2016b
		Concentration of TCE	*0.2 mg/L*	Miljøstyrelsen, 2016b
		Concentration of DCE	*4 mg/L*	Miljøstyrelsen, 2016b
		Concentration of VC	*0 mg/L*	Miljøstyrelsen, 2016b
	$k_{\_v}$	First order degradation rate PCE, TCE, DCE, VC	*0.0 day^{-1}*	JAGG 2.0
	$n_{\_v}$	Porosity	*0.3*	Miljøstyrelsen (2011)
	θ_{w_v}	Water content	*0.15*	Miljøstyrelsen (2011)
	α_{L_v}	Longitudinal dispersivity (z direction)	*0.058*	JAGG 2.0
	α_{T_v}	Transversal dispersivity (x and y direction)	*0.0058*	JAGG 2.0
	$Z_{\_v}$	Distance between the bottom of the source and the top of the aquifer	*18 m*	Miljøstyrelsen (2011)
	D_{w_v}	Free diffusion coefficient in water	7.17·10^{-10} m^2/sec	JAGG 2.0
	D_{a_v}	Free diffusion coefficient in air	7.17·10^{-6} m^2/sec	JAGG 2.0
	K_{H_v}	Henry's law constant	0.801	JAGG 2.0
	$log(K_{ow\_v})$	partition coefficient with respect to organic matter *	2.88	JAGG 2.0
	f_{oc_v}	Fraction of organic carbon PCE	0.001	JAGG 2.0
Horizontal model	H	Thickness of the aquifer	*4 m*	Miljøstyrelsen, 2016b
	u	Groundwater velocity	*40.4 m/y*	Miljøstyrelsen, 2016b
	k	First order degradation rate of PCE	*0.0005 day^{-1}*	Miljøstyrelsen, 2016b
		First order degradation rate of TCE	*0.0001 day^{-1}*	Miljøstyrelsen, 2016b
		First order degradation rate of cis-DCE	*0.0001 day^{-1}*	Miljøstyrelsen, 2016b
		First order degradation rate of VC	*0.0004 day^{-1}*	Miljøstyrelsen, 2016b
	n [-]	Porosity	*0.25*	Miljøstyrelsen, 2016b
	α_L [L]	Longitudinal dispersivity (x direction)	*1 m*	Miljøstyrelsen, 2016b
	α_T [L]	Transversal dispersivity (y direction)	*0.01 m*	Miljøstyrelsen, 2016b
	α_V [L]	Vertical dispersivity (z direction)	*0.005 m*	Miljøstyrelsen, 2016b

3.3.4 Results for MW Gjøes Vej

Figure 22 shows the PCE concentration as a function of the depth below the source (left) and at the top of the aquifer (right). Figure 22 shows that the contaminant spreads in the unsaturated zone, leading to a decrease in concentrations at the top of the aquifer.

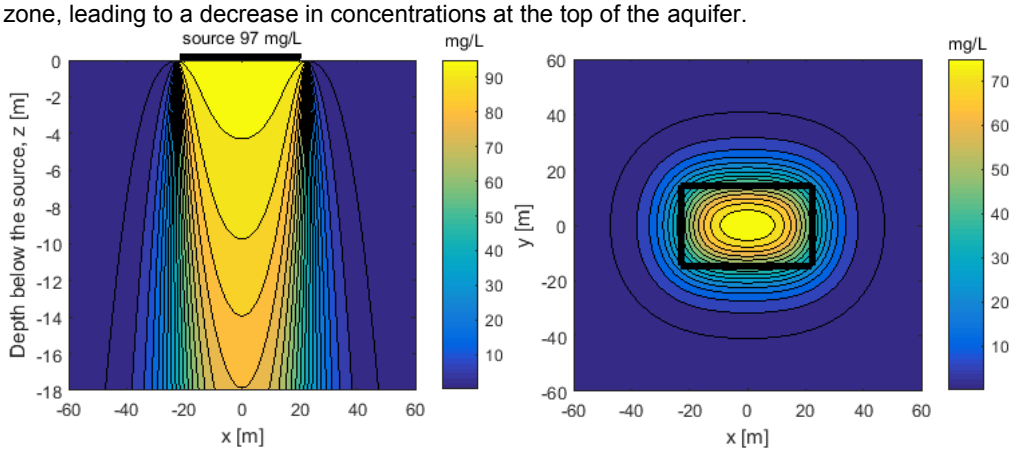

Figure 22. Concentration in a vertical cross section below the source (y=0 M) (left). Pce concentration at the top of the aquifer in plan view (right) (z_v=18 M); the black line shows the location of the contaminant source.

Figure 23 shows the concentration determined by the vertical transport model III in the unsaturated zone from the source to the top of the aquifer (18 m.b.s.). The results show about small reduction of concentration of all compounds with increasing depth below the source except for VC which is constant and equal to zero. The concentrations at the top of the aquifer (at the location *x=0* m and *y=0 m*) are about 18% smaller than the source concentrations. The reduction in concentration is due to diffusion in the gas phase (degradation is not assumed to take place because of aerobic conditions). The greater the diffusion in the gas phase is, the greater the reduction in concentrations below the source will be (the contribution of the diffusion process in the water phase is insignificant).

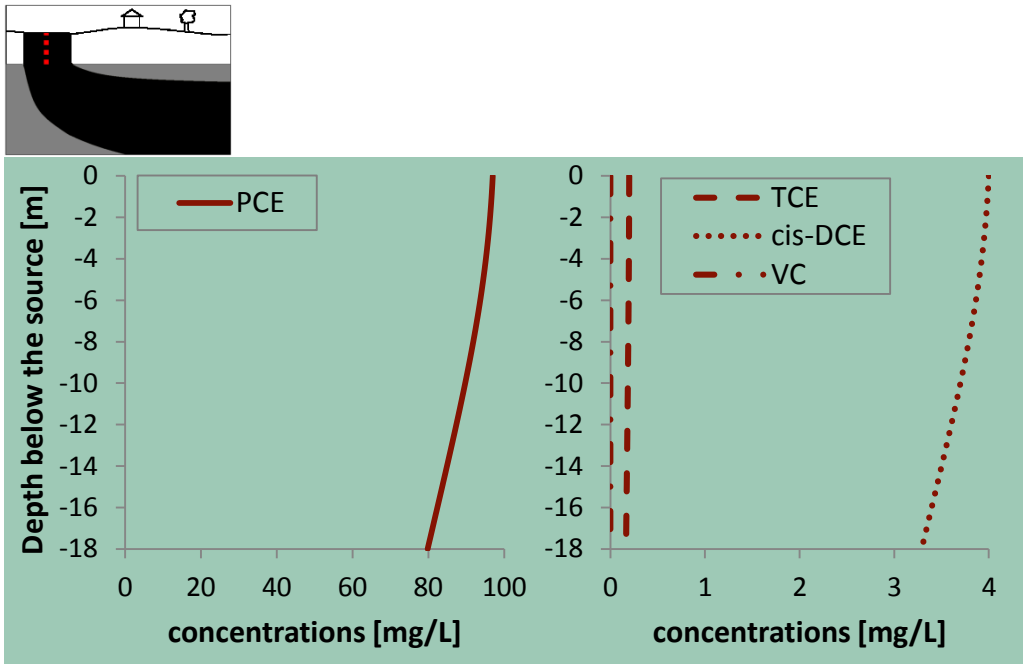

Figure 23. Concentration of PCE, TCE, cis-DCE and VC as a function of the depth below the source simulated with Model III. the level -18 m corresponds to the top of the unconfined aquifer.

The output concentration at the end of the vertical model downward pathway (the top of the aquifer) is used as input to the horizontal transport model. For instance the PCE concentration distribution at the top of the aquifer (See Figure 22 right) is integrated over the top of the aquifer (x and y axes of Figure 22 right) and multiplied by the recharge *I* rate in order to obtain the input mass discharge to the horizontal model.

Figure 24 shows the concentration of the different compounds 100 m downstream the source (100 m + Lx/2, see Figure 24 for the coordinate reference system). The concentrations are shown as a function of the depth below the groundwater table and were simulated using Model III with and without the vertical transport processes. For all the compounds the maximum concentrations obtained from Model III (with the vertical transport processes) are approximately 15% lower compared to the concentrations obtained using Model III without the vertical transport processes (only horizontal transport processes).

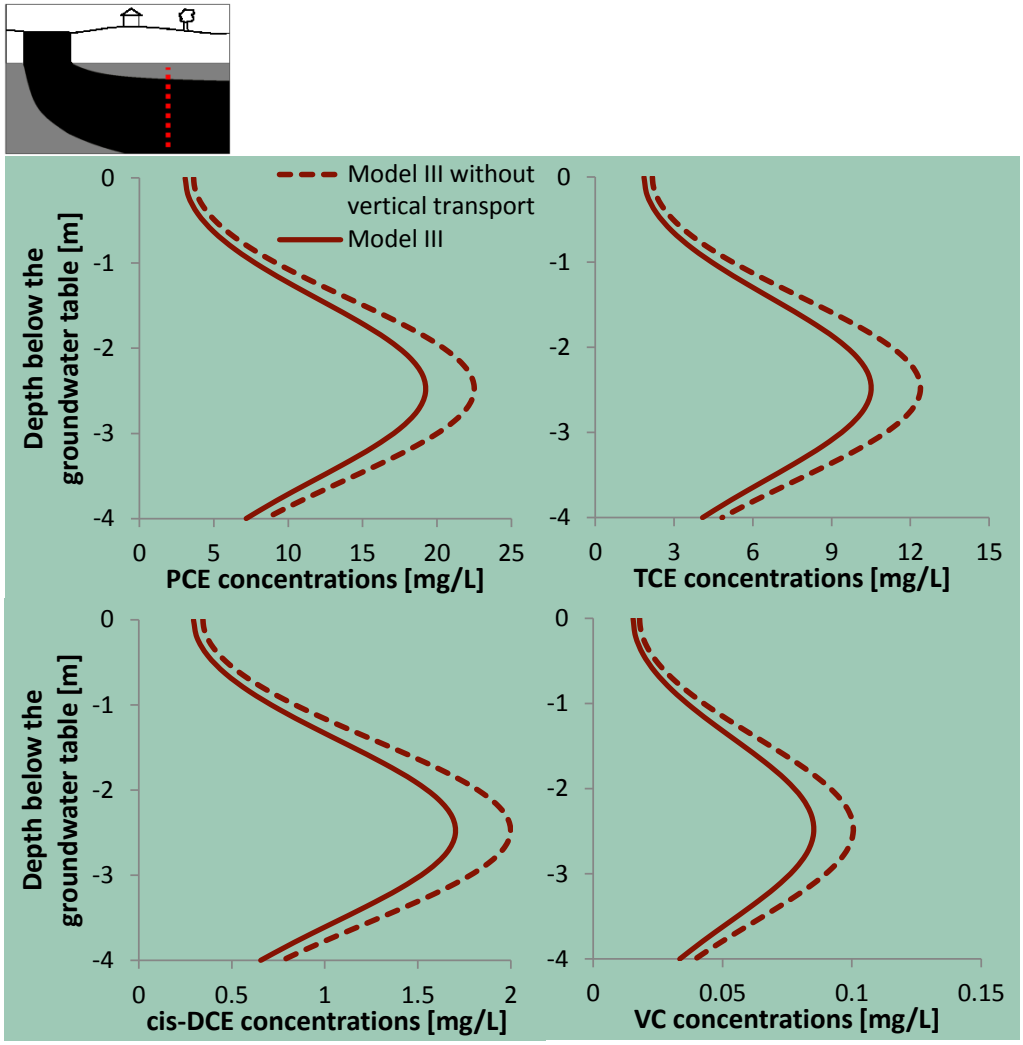

Figure 24. Contaminant concentrations 100 M downstream the source (*100 M+Lx/2*) as a function of the depth below the groundwater table. concentrations are calculated using both model III and Model III without vertical transport.

3.3.5 MW Gjøes Vej example assuming contamination of benzene and toluene

This section shows the results of a hypothetical example applying Model III to a site similar to MW Gjøes Vej, but with the chlorinated solvents replaced by the more degradable compounds benzene and toluene. Results demonstrate how changes in degradation rates change contaminant concentrations downstream the source.

The input model parameters are still as shown in Table 9 but with the following few changes applied: (1) the input concentration of benzene and toluene are assumed to be $C_{0\_v}=50\ mg/l$; (2) the free diffusion coefficient in water of benzene is $D_{w\_v}=9.3\cdot10^{-10}\ m^2/s$ and that of toluene is $D_{w\_v}=8.56\cdot10^{-10}\ m^2/s$ (JAGG 2.0); (3) the first order degradation rate of benzene (assumed to be the same both in the unsaturated and saturated zone) is $k_{\_v}=0.001\ day^{-1}$ and for toluene is $k_{\_v}=0.01\ day^{-1}$ (JAGG 2.0), so about 10-100 times higher than the ones of PCE, TCE, DCE and VC; (4) Henry's law constant benzene is $K_H=0.228$ and that of toluene $K_H=0.257$ (JAGG 2.0).

Figure 25 shows the results of the vertical transport model from the source to the top of the aquifer (18 m.b.s.) using Model III. The results show a significant reduction of concentration with increasing the depth below the source. The overall reduction of concentration is more pronounced compared to the results shown above in Figure 23 for PCE, TCE, DCE and VC. This is because toluene and benzene degrades in the unsaturated vertical transport from the source to the top of the aquifer (chlorinated solvents were assumed not to degrade in the vertical transport in the unsaturated zone due to aerobic conditions).

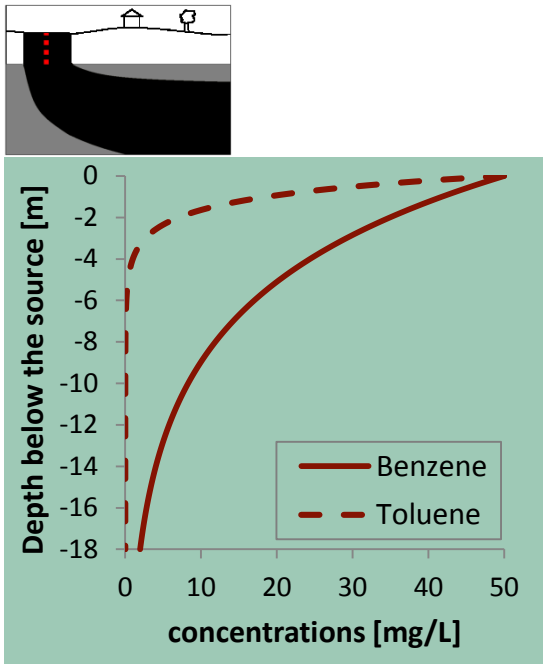

Figure 25. . Application of model iii with highly degradable compounds. concentration of benzene and toluene as a function of the depth below the source. the level -18M corresponds to the top of the aquifer.

Figure 26 shows the concentrations of benzene and toluene as a function of distance *x* in the aquifer (*y=0*) up to 100 m downstream the source. Two solutions are presented, the first one uses Model III and the second one uses Model III without the vertical transport processes (this means that the input source concentrations of benzene and toluene are directly applied to the horizontal model). The results show a significant reduction of concentration if the vertical transport processes are included.

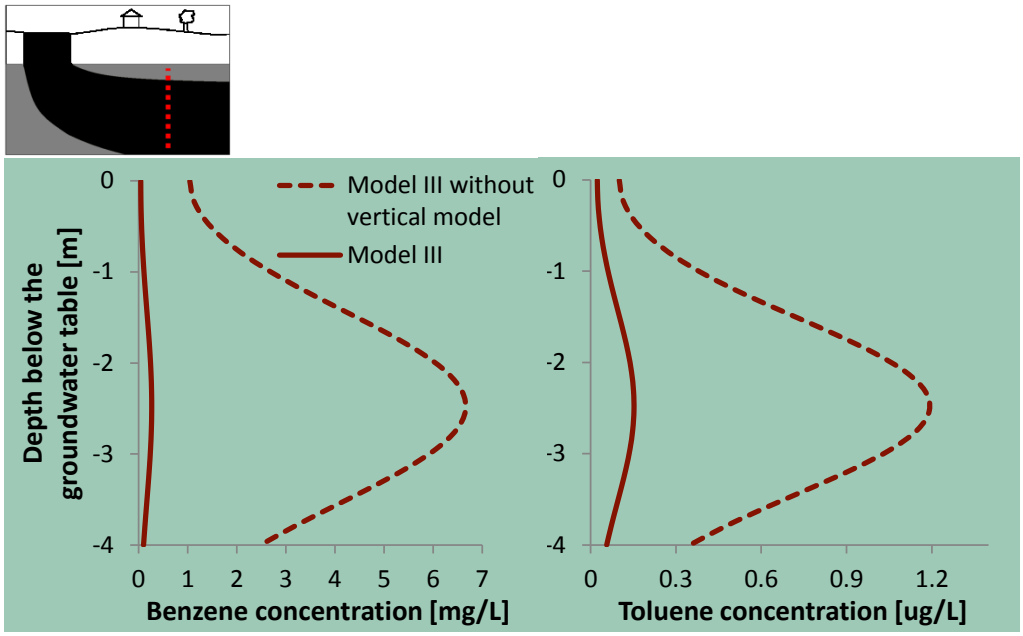

Figure 26. Model III application to easy degradable compounds. concentrations of benzene and toluene in the aquifer.

3.3.6 Determining the numerical integration intervals of Model III

In order to couple the vertical and the horizontal transport models in Model III and to determine the resulting concentrations in the aquifer downstream of the source, it is necessary to compute the integrals of Equation 8 numerically. Numerical integration from -∞ to +∞ is computationally expensive, so to reduce computational time the integration interval was selected to be from -*10·max(Lx,Ly)* to +*10·max(Lx,Ly).* In the following it is investigated how the results are influenced by the selection of different finite integration intervals and whether the selected integration interval of [-*10·max(Lx,Ly); 10·max(Lx,Ly)*] is appropriate for this case and for other contaminated sites.

Figure 27 shows the PCE mass discharge at the top of the aquifer (y-axes) as a function of different integration intervals (x-axes) and different air diffusion coefficients. These results were produced using similar parameters to MW Gjøes Vej (Table 9). Different air diffusion coefficients D_{a_v} (up to $7 \cdot 10^{-4}$ m^2/s) were used so that more volatile compounds could be included in the analysis. Results show that as the air diffusion coefficient increases, the numerical integration interval required to accurately calculate the PCE mass discharge to the top of the aquifer increases. This is because the larger the air diffusion coefficient, the greater the spreading of contaminant in space. Figure 27 shows that the integration interval *10·max(Lx,Ly)* is large enough to capture essentially all of the mass discharge at the top of the aquifer. This integration interval is specific for this case. The integration intervals are expected to increase with increasing air diffusion coefficient D_{a_v}, the distance between the source and the top of the aquifer *Z_v* and the extend of the contaminant source L_x, L_y. Nevertheless, the integration interval *10·max(Lx,Ly)* is assumed to be reasonable for other cases since this case included a high air diffusion coefficient and the distance between the source and aquifer was large (18 m).

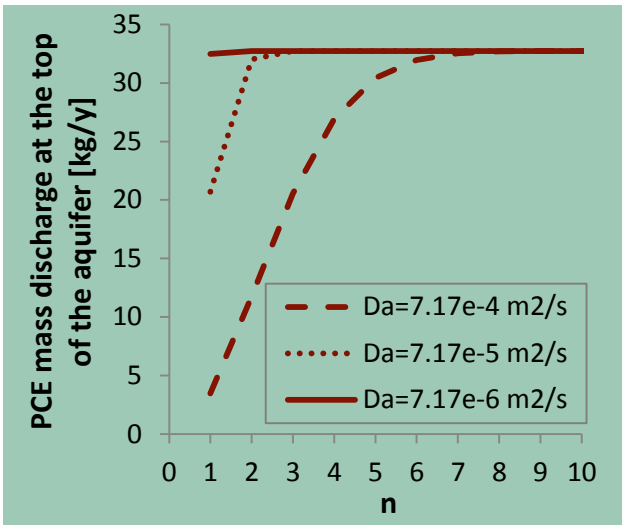

Figure 27. PCE total mass discharge at the top of the aquifer at MW Gjøes vej as a function of different integration intervals N*[MAX(LX,LY)] and Different air diffusion coefficients, *dA*.

3.3.7 Conclusion of Model III application

The results of the Model III application to MW Gjøes Vej showed the following:

- There is a 15% decrease in concentration of chlorinated solvents in the aquifer 100 m downstream of the source if the vertical transport processes are included in the model compared to when they are not.
- The vertical transport processes reduce the concentration from the source to the top of the aquifer by 18%. This is due to diffusion in the gas phase (there was no degradation in the unsaturated zone of the vertical model).
- There is a significant decrease in concentration of highly degradable compounds (benzene and toluene) in the aquifer 100 m downstream of the source if the vertical transport processes are included in the model compared to when they are not.

3.4 MW Gjøes Vej. Application of model IV

Model IV can be applied to the MW Gjøes Vej case study if the recharge in the area is assumed to be zero. The model parameters are the same as shown in Table 9 with the difference that the source is now circular with a radius of R_{source}=22.5 m and the recharge rate is set to zero (an impervious surface is assumed).

Figure 28 (left) shows the PCE concentration below the source. The results show a significant decrease of concentration with increasing horizontal distance from the source (the concentrations in the unsaturated zone are assumed constant with depth). Figure 28 (right) shows the concentration in plan view.

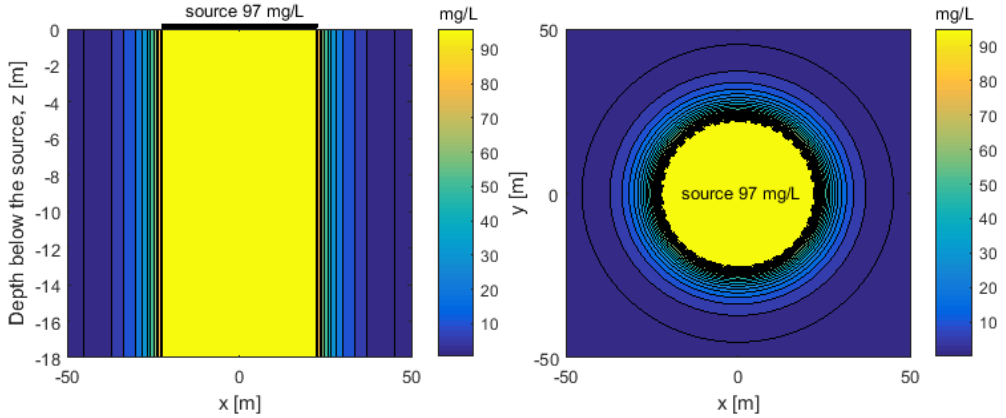

Figure 28. pce concentration in a vertical cross section (y=0 M) (left). Pce concentration at the top of the aquifer in plan view (right); the black dashed line shows the location of the contaminant source. model IV.

The output concentration at the end of the vertical model downward pathway (the top of the aquifer) is used as input to the horizontal transport model. Equation 11 is used to give the input contaminant flux to the horizontal model.

Figure 29 shows the contaminant concentration in the aquifer 100 m downstream the source (100m + R_{source}) as a function of the depth below the top of the aquifer and different capillary fringe thicknesses. Typical capillary fringe depth for sand is about 7 cm (Carsel et al., 1998). The results are also computed for doubled capillary fringe depths in order to show the influence of such model parameter. The results show that the maximum concentration is found at the top of the aquifer. This is because there is no recharge pushing the contaminant plume downward. The results also show that the larger the capillary fringe the lower the concentrations in the aquifer. This is because the larger the capillary fringe, the lower the concentration gradient between the top and the bottom of the capillary fringe, resulting in a lower water diffusive contamination flux from the unsaturated zone to the aquifer.

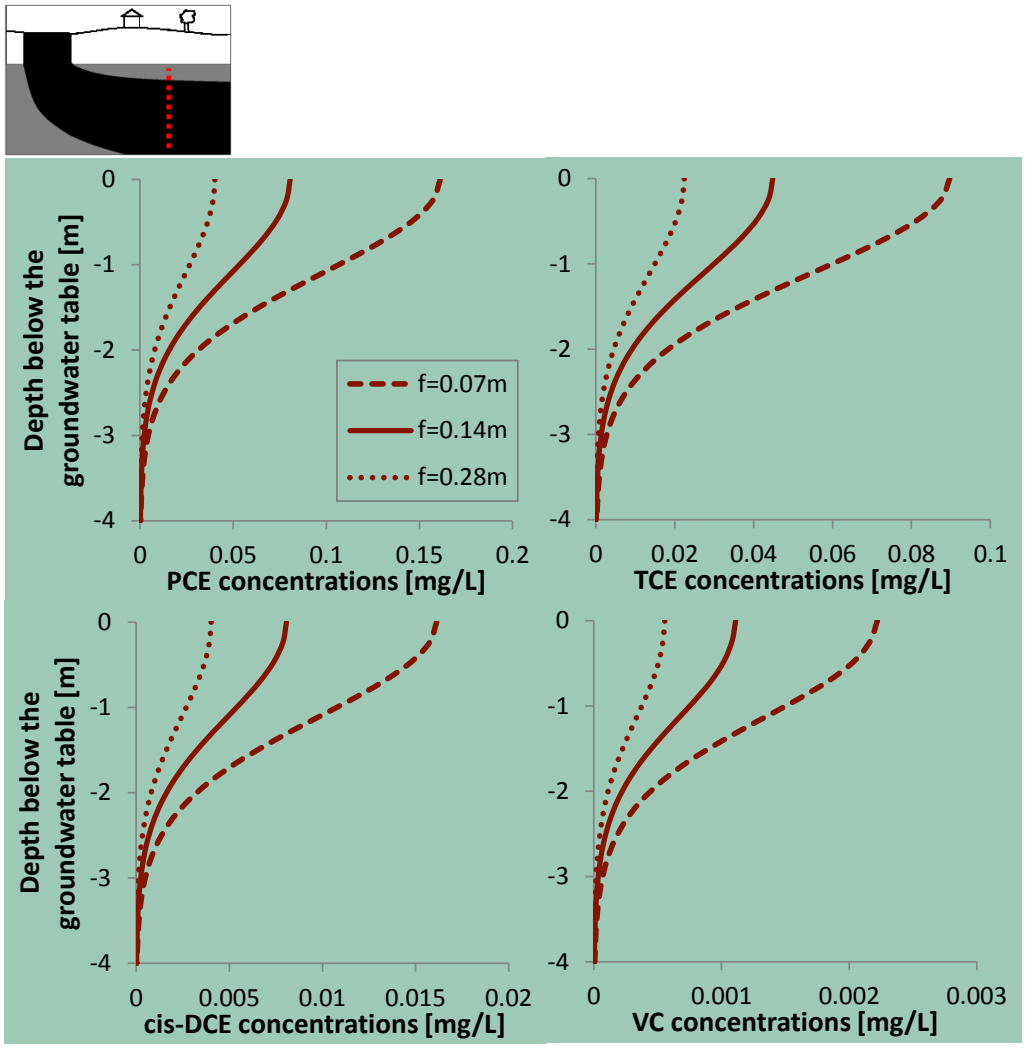

Figure 29. Contaminant concentrations in the aquifer 100 M downstream of the source (*100 M+RADIUS*) with Different capillary fringe thicknesses.

3.4.1 Determining the numerical integration intervals of Model IV.

The coupling of the vertical and the horizontal transport models in Model IV requires numerical integration of the integrals of Equation 12. Numerical integration from -∞ to +∞ is computationally demanding and the integration intervals were therefore selected to be $150 \cdot R_{source}$ where R_{source} is the radius of the contaminant source. Similar to section 3.3.5, it is investigated whether this finite integration interval is appropriate for the case here and for other cases.

Figure 30 shows the integration of the concentration distribution at the top of the aquifer as a function of different integration intervals and different air diffusion coefficients. These results were produced using the parameters for MW Gjøes Vej (Table 9).Different air diffusion coefficients D_{a_v} (up to *7e-4* m^2/s) were used so that more volatile compounds could be included in the analysis. Results show that the larger the air diffusion coefficient, the larger the integration intervals are required to be in order to accurately simulate the whole mass. This is because the larger the air diffusion coefficient, the greater the spreading of contaminant in space. Figure 30 shows that the integration interval *150·max(Radius)* is large enough to approximate all of the total contaminant mass at the top of the aquifer. This integration interval was calculated for this specific case. Nevertheless, the proposed integration interval is thought to be valid for other cases since this example employed a very large air diffusion coefficient.

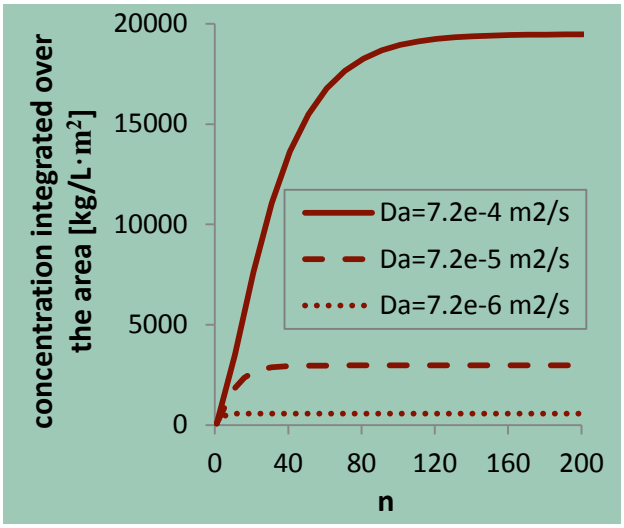

Figure 30. Concentration at the top of the aquifer at MW Gjøes vej as a function of different integration intervals N*RADIUS and different air diffusion coefficients, *dA*.

3.4.2 Conclusion of Model IV application

The results of the Model IV application to MW Gjøes Vej showed the following:

- The mass discharge to the saturated zone and the resulting concentrations in the aquifer are much smaller when there is no infiltration than when there is infiltration (Section 3.3).
- Contaminants can diffuse from the unsaturated zone to the aquifer when there is no recharge.
- The concentrations in the aquifer are very sensitive to the thickness of the capillary fringe. The thinner the capillary fringe, the greater the contaminant diffusion from the unsaturated zone to the aquifer.

References

Bear, J., 1972. Dynamics of Fluids in Porous Media. Elsevier, New York.

Broholm, K., Nilsson, B., Sidle, R.C., Arvin, E., 2000. Transport and biodegradation of creosote compounds in clayey till, a field experiment. Journal of Contaminant Hydrology, 41: 239–260.

Chambon, J., Bjerg, P.L., Binning, P.J. A risk assessment tool for contaminated sites in low-permeability fractured media. Miljøstyrelsen (udkast 2010).

Chambon, J.C., Binning, P.J., Jørgensen, P.R., Bjerg, P.L., 2011. A risk assessment tool for contaminated sites in low-permeability fractured media. Journal of Contaminant Hydrology, 124(1–4): 82-98.

Christophersen, M., Broholm, M., Mosbæk, H., Karapanagioti, H.K., Burganos, V.N., Kjeldsen, P., 2005. Transport of hydrocarbons from an emplaced fuel source experiment in the vadose zone at Airbase Værløse, Denmark. Journal of Contaminant Hydrology, vol. 81, no. 1-4, pp. 1– 33.

Christiansen, C., Wood, J. S. A., 2006. Environmental Fracturing in Clay Till Deposits, MSc thesis, Institute of Environment & Resources – Technical University of Denmark.

Grathwohl, P., Klenk, I.D., Maier, U., Reckhorn, S.B.F., 2002. Natural attenuation of volatile hydrocarbons in the unsaturated zone and shallow groundwater plumes: scenario-specific modelling and laboratory experiment. Groundwater Quality: Natural and Enhanced Restoration of Groundwater Pollution.

Hønning, J., Broholm, M.M., Bjerg, P.L., 2007. Role of diffusion in chemical oxidation of PCE in a dual permeability system. Environmental Science & Technology. 41 (24), 8426 – 8432.

JAGG 2.0. http://mst.dk/virksomhed-myndighed/jord/it-vaerktoejer-til-vurdering-af-jord/

Jørgensen, P.R., McKay, L.D., Spliid, N.H., 1998. Evaluation of chloride and pesticide transport in a fractured clayey till using large undisturbed columns and numerical modeling. Water Resources Research. 34 (4), 539–553.

Jørgensen, P.R., Hoffmann, M., Kistrup, J.P., Bryde, C., Bossi, R., Villholth, K.G., 2002. Preferential flow and pesticide transport in a clay-rich till: field, laboratory, and modeling analysis. Water Resources Research. 38 (11).

Jørgensen, T.H., Schondelmaier, A.M., Jepsen, J.D., Holm, O.V., 2003. Forureningsundersøgelse og afværgeprogram. Hovedrapport, Forurenet lokalitet nr. 461-169, Rugårdsvej 234 og 238 A-D, Odense, Fyns Amt, COWI.

Jørgensen, P.R., Helstrup, T., Urup, J., Seifert, S., 2004. Modelling of non-reactive solute transport in fractured clayey till during variable flow rate and time. Journal of Contaminant Hydrology, 68: 193-216.

Jørgensen, Torben H., Nielsen, L., Berger, H., Scheutz, C., Jakobsen, R., Bjerg, P.L., Durant, N., Cox, E., Mossing, C.H., Jacobsen, C.S., Rasmussen, P., 2007a. Forundersøgelser til pilotprojekt om stimuleret reduktiv deklorering. Miljøprojekt nr. 1146 2007. Miljøstyrelsen.

Jørgensen, Torben H., Nissen, L., Nielsen, L., Hansen, M.H., Scheutz, C., Jakobsen, R., Bjerg, P.L., Durant, N., Cox, E., Mossing, C. H., Jacobsen, C. S., Rasmussen, P., 2007b. Pilotprojekt om stimuleret reduktiv.

Klint, K.E.S., Nilsson, B., Troldborg, L., Jakobsen, P.R., 2013. A poly morphological landform approach for hydrogeological applications in heterogeneous glacial sediments. Hydrogeology Journal, 21(6), 1247–1264.

Krüger, (2004). MW Gjøes Vej, Reerslev, Supplerende undersøgelse af lerformation, Veolia Water.

Lahvis, M.A., Baehr, A.L., Baker, R.J., 2004. Evaluation of volatilization as a natural attenuation pathway for MTBE. Ground Water 42 (2), 258–267.

Lahvis, M., Rehmann, L. 2000. Simulation of Transport of Methyl Tert-Butyl Ether (MTBE) to Groundwater From Small-Volume Releases of Gasoline in the Vadose Zone. API Soil Groundwater Research Bulletin. No. 10.

Lima, G.D., Sleep, B.E., 2007. The spatial distribution of eubacteria and archaea in sand-clay columns degrading carbon tetrachloride and methanol. Journal of Contaminant Hydrology 94, 34 – 48.

Lu, C., Bjerg, P. L., Zhang, F., Broholm, M.M., 2011. Sorption of chlorinated solvents and degradation products on natural clayey tills. Chemosphere, 83(11), 1467–1474.

McKay, L.D., Cherry, J.A., Gillham, R.W., 1993. Field experiment in a fractured clay till. 1. Hydraulic conductivity and fracture aperture. Water Resources Research Vol. 29, No. 4: 1149-1162.

Miljøstyrelsen, 1998. Oprydning på forurenede lokaliteter, Hovedbind og Appendiks. Vejledning fra Miljøstyrelsen nr. 6 og 7, 1998.

Miljøstyrelsen, 2002. Vejledning om overgangsplaner. Udarbejdelse af overgangsplaner for bestående Deponeringsanlæg. Vejledning fra Miljøstyrelsen Nr. 5 2002.

Miljøstyrelsen, 2009a. A risk assessment tool for contaminated sites in low-permeability fractured media. Environmental project No. 1786, 2015.

Miljøstyrelsen, 2009b. Model assessment of reductive dechlorination as remediation technology for contaminant sources in fractured clay. Case studies. Delrapport III. Environmental Project No. 1296 2009. Miljøprojekt.

Miljøstyrelsen, 2011. Fastlæggelse af oprensningskriterier for grundvandstruende forureninger. Miljøprojekt nr.137, 2011.

Miljøstyrelsen, 2013. Manual for program til risikovurdering – JAGG 2.0. Miljøprojekt nr. 1508, 2013.

Miljøstyrelsen, 2014. Liste over kvalitetskriterier i relation til forurenet jord og kvalitetskriterier for drikkevand. Opdateret maj 2014. Miljøministeriet, Miljøstyrelsen.

Miljøstyrelsen, 2015. A risk assessment tool for contaminated sites in low-permeability fractured media. Environmental project No. 1786.

Miljøstyrelsen, 2016a. JAGG 2 - Vertikal transport ned til førstkommende betydende magasin. Miljøprojekt nr. 1828, 2016.

Miljøstyrelsen, 2016b. GrundRisk Beregningsmodel til risikovurdering af grundvandstruende forureninger. Miljøprojekt nr. 1865, 2016.

Niras, 2009. MW Gjøes Vej, Reerslev, Indsamling, systematisering og vurdering af data, Koncern Miljø, Region Hovedstaden.

Parker, B.L., Gillham, R.W., Cherry, J.A., 1994. Diffusive disappearance of immiscible-phase organic liquids in fractured geologic media. Ground Water. 32 (5), 805–820.

Scheutz, C., Durant, N.D., Dennis, P., Hansen, M.H., Jørgensen, T., Jakobsen, R., Cox, EE., Bjerg, P.L., 2008. Concurrent Ethene Generation and Growth of Dehalococcoides Containing Vinyl Chloride Reductive Dehalogenase Genes During an Enhanced Reductive Dechlorination Field Demonstration. Environmental Science & Technology 42 (24), s. 9302-9309.

Scheutz, C., Broholm, M.M., Durant, N.D., Weeth, E.B., Jørgensen, T.H., Dennis, P., Jacobsen, C.S., Cox, E.E., Chambon, J.C., Bjerg, P.L., 2010. Field evaluation of biological enhanced reductive dechlorination of chloroethenes in clayey till. Environmental Science & Technology. 44 (13), 5134–5141.

Schwarzenbach, R.P., Gschwend, P.M., Imboden, D.M., 1993. Environmental Organic Chemistry. John Wiley & Sons, INC.

Spiegel, M.R. (1968): Mathematical handbook of formulas and tables. Schaum's outline series. McGraw-Hill.

Sun, Y., Petersen, J.N., Clement T.P., 1999a. Analytical solutions for multiple species reactive transport in multiple dimensions, Journal of Contaminant Hydrology, 35(4), 429-440.

Sun, Y., Petersen, J.N., Clement T.P., Skeen R.S., 1999b. Development of analytical solutions for multispecies transport with serial and parallel reactions, Water Resources Research, 35(1), 185-190.

Tang, D.H., Frind, E.O., Sudicky, E.A., 1981. Contaminant transport in fractured porous-media — analytical solution for a single fracture. Water Resources Research. 17 (3), 555–564.

Troldborg, M., Binning, P.J., Nielsen, S., Kjeldsen, P., Christensen, A.G., 2009. Unsaturated zone leaching models for assessing risk to groundwater of contaminated sites. Journal of hydrology. Volume 105, Issues 1–2.

Van Genuchten, M.T, Alves, W.J., 1982. Analytical Solutions of the One Dimensional Convective-Dispersive Solute Transport Equation. United States Department of Agriculture. Agricultural research Service. Technical Bulletin, Number 1661.

Videncenter for Jordforurening, 2008. SprækkeJAGG. Regneark til risikovurdering af sprækker i moræneler Teknik og Administration Nr. 2, 2008.

Wexler, E.L., 1992. Analytical Solutions for one-, two- and three-dimensional solute transport in ground-water systems with uniform flow. Chapter B7 in Techniques of Water-Resources Investigations of the United States Geological Survey. Book 3 Applications of Hydraulics. U.S. Department of the interior. U.S. Geological Survey. United States Government Printing Office, 1992.

Appendix I

This section discusses the effect of different sorption characteristics of different soil types on contaminant transport simulations that cross different soil layers. A 1D COMSOL Multyphisics model was setup to support our discussion. Figure 31 (top) a shows the conceptual model set-up. An inflow contaminant flux is applied to the left boundary, the flux crosses both 'soil type 1' and 'soil type 2' ('soil type 2' has a higher partition coefficient K_d) and then it outflows through the right boundary. The following transport equation is solved:

$$R\frac{\partial C_w}{\partial t} = D_w \nabla^2 C_w - v\frac{\partial C_w}{\partial x}$$

The diffusion coefficient D_w and the veolocity v were equal for both soil types, however the retardation factor R ($R=1+\rho_b \cdot K_d/n$) was lower for 'soil type 1' compare to 'soil type 2' because 'soil type 1' has a lower partition coefficient K_d.

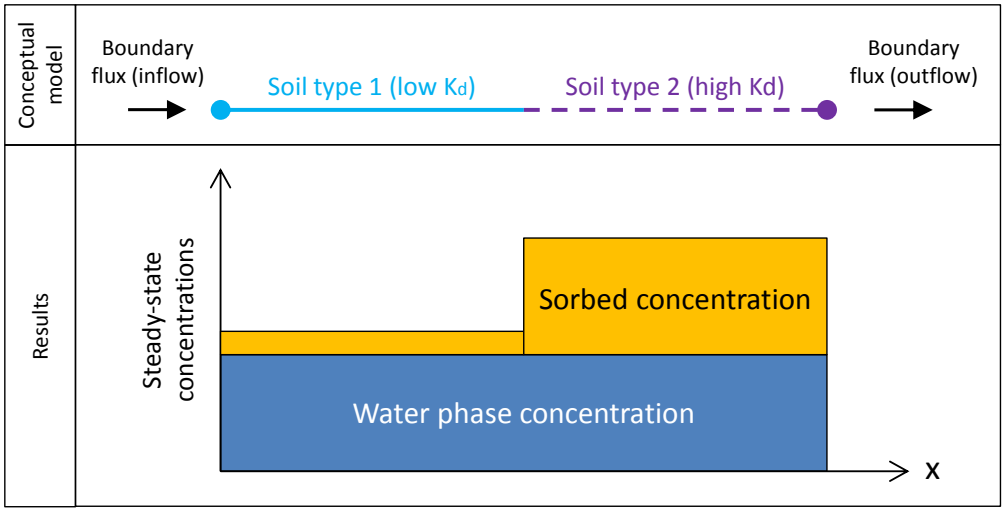

FIGURE 31. (TOP) CONCEPTUAL MODEL A HORIZONTAL CONTAMINANT FLUX ENTER THE SOIL TYPE 1 FROM THE LEFT END, IT CROSSES BOTH THE 2 SOIL TYPES AND THEN IT OUTFLOWS THROUGH THE RIGHT BOUNDARY. (BOTTOM) RESULTS. THE WATER PHASE CONCENTRATION IS THE SAME IN THE 2 SOIL TYPES, HOWEVER THE SORBED CONCENTRATIONS ARE HIGHER IN SOIL TYPE 2 WHICH HAS A HIGHER DISTRIBUTION COEFFICIENT Kd.

Figure 31 (bottom) a shows the steady state results of the simulation. The results show that the water phase concentrations are the same in the 2 different soil types, however the sorbed concentrations vary depending on the sorption characteristics of the soil.

Based on the results of the model we can conclude that:

- A jump in the retardation factor R changes the contaminant velocity.
- There is no jump in aqueous concentration at the boundaries between materials. At the boundary between two materials, the upstream aqueous flow hits the new downstream material. At that point, the sorption sites fill up until they reach equilibrium with the incoming solution (with the upstream aqueous concentration).
- There is a jump in sorbed concentration at the boundaries between materials. If the concentration c is fixed, and the sorbed concentration $S=k_d \cdot c$, then a jump in k_d leads to a jump in S.

- The two materials will have different total concentrations (total contaminant mass/volume) at steady-state because of the change in sorption characteristics.

GrundRisk – Coupling of vertical and horizontal transport models

This report presents the development of the GrundRisk model for contaminated site risk assessment. GrundRisk consists of 5 models, each simulating the contaminant transport from a contaminant source to an underlying aquifer. Each model consist of a vertical transport model (based on the models presented in Miljøstyrelsen (2016a)) coupled to a horizontal transport model (Miljøstyrelsen (2016b). This report focuses on the coupling between the vertical and horizontal models.

Environmental
Protection Agency
Strandgade 29
DK-1401 København K

www.mst.dk